Check for updates

Received: 5 August 2022 | Revised: 9 September 2022 | Accepted: 19 September 2022

DOI: 10.1111/pce.14448

ORIGINAL ARTICLE

Plant, Cell & Environment PC&E WILEY

Vertical gradients in photosynthetic physiology diverge at the latitudinal range extremes of white spruce

Stephanie C. Schmiege[1,2,3,4] | Kevin L. Griffin[1,5,6] | Natalie T. Boelman[6] | Lee A. Vierling[7,8] | Sarah G. Bruner[1] | Elizabeth Min[5] | Andrew J. Maguire[7,8] | Johanna Jensen[1] | Jan U. H. Eitel[7,8]

[1]Department of Ecology, Evolution and Environmental Biology, Columbia University, New York, New York, USA

[2]New York Botanical Garden, Bronx, New York, USA

[3]Plant Resilience Institute, Michigan State University, East Lansing, Michigan, USA

[4]Department of Biology, Western University, London, Ontario, Canada

[5]Department of Earth and Environmental Sciences, Columbia University, Palisades, New York, USA

[6]Lamont-Doherty Earth Observatory, Columbia University, Palisades, New York, USA

[7]Department of Natural Resources and Society, College of Natural Resources, University of Idaho, Moscow, Idaho, USA

[8]McCall Outdoor Science School, College of Natural Resources, University of Idaho, McCall, Idaho, USA

Correspondence

Stephanie C. Schmiege, Plant Resilience Institute, Michigan State University, East Lansing, Michigan 48824, USA.
Email: schmie18@msu.edu

Funding information

NASA ABoVE, Grant/Award Number: NNX15AT86A; National Science Foundation, Grant/Award Numbers: 1637459, 2220863; Plant Resilience Institute, Michigan State University

Abstract

Light availability drives vertical canopy gradients in photosynthetic functioning and carbon (C) balance, yet patterns of variability in these gradients remain unclear. We measured light availability, photosynthetic CO_2 and light response curves, foliar C, nitrogen (N) and pigment concentrations, and the photochemical reflectance index (PRI) on upper and lower canopy needles of white spruce trees (*Picea glauca*) at the species' northern and southern range extremes. We combined our photosynthetic data with previously published respiratory data to compare and contrast canopy C balance between latitudinal extremes. We found steep canopy gradients in irradiance, photosynthesis and leaf traits at the southern range limit, but a lack of variation across canopy positions at the northern range limit. Thus, unlike many tree species from tropical to mid-latitude forests, high latitude trees may not require vertical gradients of metabolic activity to optimize photosynthetic C gain. Consequently, accounting for self-shading is less critical for predicting gross primary productivity at northern relative to southern latitudes. Northern trees also had a significantly smaller net positive leaf C balance than southern trees suggesting that, regardless of canopy position, low photosynthetic rates coupled with high respiratory costs may ultimately constrain the northern range limit of this widely distributed boreal species.

KEYWORDS

Arctic treeline, canopy gradients, carbon balance, photochemical reflectance index, photosynthesis, *Picea glauca*

This is an open access article under the terms of the Creative Commons Attribution-NonCommercial-NoDerivs License, which permits use and distribution in any medium, provided the original work is properly cited, the use is non-commercial and no modifications or adaptations are made.
© 2022 The Authors. *Plant, Cell & Environment* published by John Wiley & Sons Ltd.

1 | INTRODUCTION

Illuminating the factors driving species' distributional ranges, that is, the boundaries within which a species can grow and reproduce successfully, remains a fundamental ecological, evolutionary and biogeographic challenge. Extensive research has uncovered a number of factors that play important roles. These include environmental tolerance, niche breadth, metapopulation dynamics, genetic diversity, phenotypic plasticity and dispersal ability (Brown et al., 1996; Gaston, 1996; Lowry & Lester, 2006). The diversity of possible factors highlights that no universal cause of species' distributions has yet emerged, but rather that a combination of historical, physiological and biotic filters may define a species' distributional range (Lambers & Oliveira, 2019). Nevertheless, the ability of a plant to tolerate the local growth environment remains paramount. This ability is intimately linked to a species' physiological performance. The physiological processes of photosynthesis and respiration, resulting in the exchange of carbon, are heavily affected by environmental conditions. Together, these two processes determine the carbon balance of a plant which must remain positive if a plant is to grow, survive and reproduce in a given environment. Thus, photosynthesis and respiration fundamentally act as a physiological filter determining a species' distributional range (Lambers & Oliveira, 2019). They are also critical to quantifying carbon exchange as well as the ecological effects of climate change on future carbon sequestration.

The evolution from modelling vegetation as a single 'big leaf' to 'two big leaves' including distinct parameters for sun and shade leaves, to multilayer canopies including gradients of physiological function (Field, 1983; Sands, 1995) has improved estimates of vegetative carbon gain in many ecosystems (Bonan et al., 2012; Harley & Baldocchi, 1995; de Pury & Farquhar, 1997; Rogers et al., 2017). These multilayer canopy models are parameterized using physiological and biochemical traits that vary predictably with vertical gradients in environmental conditions such as light, temperature, humidity and vapour pressure deficit throughout the tree crown (Bond et al., 1999; Sellers et al., 1992). Of particular importance to modelling photosynthesis are gradients in light availability. For example, traits such as maximum photosynthesis (A_{max}) and leaf nitrogen content, as well as leaf mass per area have been found to correlate positively with changes in irradiance (Ellsworth & Reich, 1993; Field, 1983; Hirose & Werger, 1987; Niinemets, 2007; Niinemets et al., 1998) leading to the common finding that high canopy, high light foliage has higher photosynthetic capacity. Pigment pools have similarly been found to vary with canopy position and irradiance with high light foliage frequently containing larger pools of photoprotective pigments that can dissipate excess light energy and protect chlorophyll-filled photosystems (Demmig-Adams & Adams, 1992). Even the ratio of Chla:Chlb frequently reflects canopy gradients of light availability because shade-adapted leaves contain more light harvesting antenna complexes (LHCII) associated with photosystem II that are high in Chlb (Dale & Causton, 1992; Hikosaka & Terashima, 1995; Kitajima & Hogan, 2003; Magney et al., 2016; Ruban, 2015; Scartazza et al., 2016). Thus, the incorporation of canopy gradients into carbon exchange modelling comes from a strong foundation of work that demonstrates how differences in photosynthetic functioning and resource allocation depend on canopy position and light availability.

Other environmental factors may also play a role in determining canopy gradients in photosynthesis. For example, photosynthesis is not only dependent on light availability, but also on water transport to leaves since high photosynthetic rates tend to require high rates of stomatal conductance and transpiration (Schulze et al., 1994; Wong et al., 1978). Thus, limitations in water availability may constrain vertical canopy gradients even if light is available in abundance, resulting in shallower canopy gradients in photosynthesis and leaf nitrogen (Peltoniemi et al., 2012). Therefore, we cannot assume that light availability is the only driver of canopy gradients without quantifying its effect on photosynthesis, especially in species whose ranges span large latitudinal differences over which environmental conditions can vary dramatically. In this study we examine the strength of the relationships between light availability and canopy gradients of physiological traits across the range extremes of an important boreal species.

White spruce [*Picea glauca* (Moench) Voss] has a massive, transcontinental range distribution stretching from the forest tundra ecotone (FTE) in northern Alaska where it is one of the dominant species, to mixed forests on the eastern seaboard of Canada and New England (Eitel et al., 2019; Thompson et al., 2015; Viereck et al., 1986). At the northern edge of the distribution, white spruce are exposed to unique environmental challenges for plant growth and survival including low winter temperatures, shallow soil depth underlain by permafrost and brief growing seasons. During the growing season, white spruce canopies are exposed to a unique light environment caused by high solar zenith angles and continuous photoperiod (i.e., 24 h of light for several weeks). Furthermore, tree crown structure at the FTE exhibits an almost ubiquitous tall, vertical, narrow and untapering crown shape (Kuuluvainen, 1992) which creates an open canopy forest structure with widely spaced trees. By contrast, white spruce at the southern range extreme are exposed to much lower solar zenith angles and a shorter photoperiod during the growing season. The southern tree crowns are also generally much denser, wider and more tapered and typically grow with a higher stand density than in the north. These contrasting light environments may impact canopy gradients of light interception, which may, in turn, drive canopy gradients of photosynthetic physiology, biochemistry and pigment concentrations.

In addition to photosynthetic, biochemical and pigment traits, we also examine canopy differences in the photochemical reflectance index (PRI). This index is a more successful photosynthetic proxy than the commonly used normalized difference vegetation index in conifer species because it is sensitive to changes in pigment pools such as the ratio of chlorophylls to carotenoids (Gamon et al., 2016). PRI has been successfully employed to track seasonal changes in photosynthetic phenology in coniferous forests (Gamon et al., 2016; Wong & Gamon, 2015a, 2015b) and at the FTE (Eitel et al., 2019, 2020), and a broadband analog chlorophyll carotenoid index, can be derived from global Moderate Resolution Imaging Spectroradiometer imagery (Gamon et al., 2016). Thus, PRI presents a promising prospective

13653040, 2023, 1, Downloaded from https://onlinelibrary.wiley.com/doi/10.1111/pce.14448 by Columbia University Libraries, Wiley Online Library on [05/09/2024]. See the Terms and Conditions (https://onlinelibrary.wiley.com/terms-and-conditions) on Wiley Online Library for rules of use; OA articles are governed by the applicable Creative Commons License

avenue for further understanding carbon dynamics across broadly distributed conifer forests.

In this study we focus specifically on the photosynthetic traits of white spruce and their relationship to light environment. However, to gain a full picture of the physiological limits at latitudinally distant range extremes, a carbon balance approach should be employed. In fact, recent work on the physiology of white spruce has focused specifically on the respiratory cost associated with growth and survival at the FTE. In a previous study, we found that white spruce in this environment have extremely high respiration compared to white spruce growing at the southernmost range extreme as well as higher respiration than the average respiration of the boreal biome and needle-leaved evergreen trees (Griffin et al., 2021). Griffin et al. (2021) posit that this high respiratory cost may constrain the northern limit of white spruce and the Arctic treeline in general. With the addition of photosynthetic traits measured on the same trees, we are now in a unique position to examine the degree to which this respiratory cost is matched by photosynthetic carbon gains and whether a lower carbon balance may contribute to the northern limits of white spruce's latitudinal range.

Thus, the overarching aims of this study are twofold: firstly, to provide a comprehensive assessment of the photosynthetic physiology of white spruce and its relationship to canopy and latitudinal light environment at its range extremes; and secondly, to examine whether the leaf carbon balance of this species constrains its northernmost range limit. Firstly, we hypothesize that foliar light availability, physiological traits, biochemical traits and PRI will converge across high and low vertical canopy positions in white spruce growing at the FTE. In contrast, steep canopy gradients of light availability and all foliar traits will be apparent at the southernmost range extreme. Secondly, we hypothesize that the carbon balance of white spruce at the northern location will be much lower than the southern location reflecting the challenging growth environment and providing a physiological mechanism for the northernmost range extreme of this important boreal species.

2 | MATERIALS AND METHODS

2.1 | Site descriptions

This study was conducted in two locations at the northern and southern range extremes of white spruce [*P. glauca* (Moench) Voss]. In the north, data were collected from six sites chosen to represent the FTE (Eitel et al., 2019). These sites are located along a 5.5 km long stretch of the Dalton Highway, in the Brooks Range in northern Alaska (67°59′40.92″ N latitude, 149°45′15.84″ W longitude). At the FTE, white spruce is the dominant tree species with deciduous shrubs and sedges present in the understory (Eitel et al., 2019). The forest structure is relatively open with approximately 407 stems ha^{-1} (Jensen pers. comm.). Three white spruce study trees with diameter at breast height (DBH) greater than 10 cm were chosen at each site for a total of 18 study trees at the FTE (tree characteristics are described in Table 1). Mean annual precipitation was 485.4 mm and mean annual temperature was −8.1°C as determined from a SNOTEL site at the nearby Atigun Pass (https://wcc.sc.egov.usda.gov/nwcc/site?sitenum=957) between 2007 and 2016. During the Alaska measurement campaign in July 2017, photoperiod ranged from 22 to 24 h. All measurements were taken at a high and low south-facing canopy position on each of 18 trees for a total of 36 measurements. The low canopy position was at approximately 1.37 m (DBH), and the high canopy position was approximately 1 m below the apical meristem.

TABLE 1 Means ± 1 standard error for characteristics of trees from the forest tundra ecotone (FTE), Alaska (n = 18) and Black Rock Forest (BRF), New York (n = 6), including diameter at breast height (DBH; cm), tree height (m), dripline area (m^2), stems per hectare (means only, as reported in Whitehead et al. (2004) for BRF and from Jensen pers. comm. for the FTE)

Location	DBH (cm)	Tree height (m)	Dripline area (m^2)	Stems ha^{-1}
BRF	23.10 (1.99)	9.91 (0.73)	27.34 (2.00)	760
FTE	16.71 (0.94)	9.32 (0.57)	3.52 (0.37)	407

At the southern edge of the species' range, data were collected from six trees located in Black Rock Forest (BRF), New York (BRF; 41°24′03.91″ N latitude, 74°01′28.49″ W longitude; Table 1). BRF is an oak-dominated forest with approximately 760 stems ha^{-1} (Whitehead et al., 2004). Mean annual precipitation from 1982 to 2010 was 1285 mm and mean annual temperature was 10.9°C (Arguez et al., 2012). During our BRF measurement campaign in June 2017, photoperiod was approximately 15 h. BRF is an oak-dominated northern temperate deciduous forest (Patterson et al., 2018; Schuster et al., 2008). Measurements were also taken at high and low south-facing canopy positions on each tree. Due to the lower count of available trees, 3 measurements were taken at the low and high canopy positions on each of the six trees for a total of 36 measurements. As at the FTE, the low canopy position was at approximately 1.37 m and the high canopy position was approximately 1 m below the apical meristem.

2.2 | Environmental measurements

Hemispherical photographs were taken with a digital camera (CoolPix 4500; Nikon Corporation) and an attached fisheye lens to assess canopy openness at the high and low canopy positions chosen for each tree (described above). The camera was positioned immediately adjacent to the branch chosen for measurements, with the camera pointing north. Once the camera was level, the hemispherical canopy photo was taken. Using these photographs, light environment was assessed and modelled using the free R code and documentation of ter Steege (2018). These scripts are based on the widely used Hemiphot and Winphot programmes (ter Steege, 1993, 1997). Modelling of the light environment using this code takes into

13653040, 2023, 1, Downloaded from https://onlinelibrary.wiley.com/doi/10.1111/pce.14448 by Columbia University Libraries, Wiley Online Library on [05/09/2024]. See the Terms and Conditions (https://onlinelibrary.wiley.com/terms-and-conditions) on Wiley Online Library for rules of use; OA articles are governed by the applicable Creative Commons License

account GPS location as well as the measurement dates to correct for differences in solar angle (see ter Steege (2018) for a fuller description). Average photosynthetic photon flux density (PPFD; mol m^{-2} day^{-1}) at the high and low canopy positions was calculated by averaging the diurnal light courses over the measurement campaign days (June 21 to June 27 at BRF, and July 4 to July 20 at the FTE). At the FTE, air temperature (°C) was collected using a meteorological sensor (VP-4; METER) and local solar open sky radiation readings were collected using a PYR Solar Radiation Sensor (METER). Solar radiation (W m^{-2}) was converted to PPFD (μmol m^{-2} s^{-1}) by multiplying by 2.02 (Mavi & Tupper, 2004). At BRF, air temperature and local open sky PPFD were collected from a nearby BRF-run weather station (https://blackrock.ccnmtl.columbia.edu/portal/weather/) equipped with a temperature/humidity sensor (HC2S3; Rotronic) and a quantum sensor (LI-190SB Quantum Sensor; LI-COR).

2.3 | Gas exchange measurements

Gas exchange was measured at high and low canopy positions on each tree at the two locations. At both locations, measurements were taken on a branch tip inserted into the cuvette. At BRF, all measurements were taken on the tree with high canopy reached using an articulating boom lift (600AJ; JLG). At the FTE, low canopy branches were measured on the tree, but high canopy branches had to be detached using a pole-clippers (Fiskars fiberfill pole pruner; Fiskars Brands Inc.) as there was no way to reach samples otherwise. Detaching foliage for physiological measurements is common, with no observable differences usually found between attached and detached samples (Akalusi et al., 2021). For detached samples, cut branches at least 30 cm in length were placed immediately in water, and recut underwater. All measurements on cut branches were taken within 12 h. CO_2 (A-C_i) and light response (A-Q) curves were collected using two portable photosynthesis systems (LI-6800; LI-COR). Needles were sealed in a cuvette in which the temperature and relative humidity were set to 20°C and 50% humidity at the FTE, and 25°C and 60% humidity at BRF to mirror ambient conditions in each location. For the A-C_i curves, irradiance was kept constant at 1000 PPFD and the CO_2 concentrations were stepped through the following concentrations (ppm): 1200, 1000, 800, 600, 400, 300, 200, 100, 75, 50, 25, 0. Values of V_{cmax} (the maximum rate of RuBisCO carboxylation) and J_{max} (the maximum rate of electron transport) were determined according to the photosynthesis model of Farquhar, von Caemmerer and Berry (Farquhar et al., 1980) and adjusted to 25°C using the plantecophys package in R (Duursma, 2015).

For the A-Q curves, reference CO_2 concentration was set to 400 ppm and photosynthesis was measured at the light intensities: 1800, 1500, 1200, 1000, 800, 400, 200, 150, 100, 90, 80, 75, 70, 65, 60, 55, 50, 45, 40, 35, 30, 25, 20, 15, 10, 5, 0 μmol m^{-2} $s.^{-1}$ After 15 min at zero irradiance, respiration in the dark (R_D) was recorded. Maximum likelihood estimation [executed in the bblme package for R (Bolker & R Development Core Team, 2020)] was used to fit the following model (describing a non-rectangular hyperbola) to the data (Herrmann et al., 2020):

$$A = \frac{\Phi^{*}I + A_{max} - \sqrt{(\Phi^{*}I + A_{max})^2 - 4^{*}\theta^{*}\Phi^{*}I^{*}A_{max}}}{2^{*}\theta} - R_D$$

where, A is the measured rate of photosynthesis, θ is the curvature factor and I is the irradiance. Parameters extracted and calculated from the fit of the model to each light curve included the maximum rate of CO_2 fixation (A_{max}), photosynthesis at 1500 μmol m^{-2} s^{-1} (A_{1500}), the apparent quantum yield (Φ), the light compensation point (LCP, the light level required for zero net carbon flux) and the light saturation point (LSP, the light level required to obtain 75% of A_{1500}).

2.4 | Respiration in the light

Respiration in the light (R_L) was obtained from the A-Q curves according to the methods of Kok (1948); Sharp et al. (1984); and Heskel et al. (2013). These curves contain a subtle change in slope near the light compensation point (the light intensity where photosynthesis and respiration equal each other). The break point where this change in slope occurs divides the photosynthetic response to light into two linear sections. Extrapolating from the upper linear portion of the curve to the y-axis highlights an alternate respiration value which was interpreted by Bessel Kok to be the amount of respiration occurring in the light (Heskel et al., 2013; Kok, 1948; Tcherkez et al., 2017).

An important assumption of the Kok method is that carbon assimilation is only influenced by light. Consequently, corrections were made to account for any changes in internal CO_2 concentration (C_i) following the methods of Kirschbaum and Farquhar (1987) [see Ayub et al. (2011) for a full description]. It is possible that R_L measured with the Kok method may be influenced by factors such as mesophyll conductance (*n.b.* Buckley et al., 2017; Farquhar & Busch, 2017); however, such investigations are beyond the scope of this study.

2.5 | Leaf trait measurements

After collecting A-C_i and A-Q curves, needles were detached from the branch, photographed to determine projected surface area (cm^2) using ImageJ (Schneider et al., 2012), placed into coin envelopes and oven dried at 60°C for 48 h. Leaves were reweighed postdrying for leaf dry mass (g). Specific leaf area (SLA; cm^2g^{-1}) was calculated. Leaf samples were then ground using a ball mill (SPEX 8000 Mixer/Mill) and prepared for analysis of % carbon and % nitrogen using a carbon-nitrogen flash analyser (CE Elantech). Using these percentages, foliar nitrogen per area (N_{area}; mg cm^{-2}) and the carbon to nitrogen ratio (C:N) were calculated.

13653040, 2023, 1, Downloaded from https://onlinelibrary.wiley.com/doi/10.1111/pce.14448 by Columbia University Libraries, Wiley Online Library on [05/09/2024]. See the Terms and Conditions (https://onlinelibrary.wiley.com/terms-and-conditions) on Wiley Online Library for rules of use; OA articles are governed by the applicable Creative Commons License

2.6 | Pigment measurements

Needles growing on branches adjacent to those selected for gas exchange at both high and low canopy positions were selected for pigment analysis. Branches were wrapped in wet paper towels and foil, and transported back to the laboratory in a cooler with ice. Foliar pigment extraction began no later than 3 h after returning from the field, and any samples not processed in this time were frozen until pigment extraction could take place.

Between 5 and 10 needles were removed from each branch and their wet weight and needle area measured. Needles were ground in 100% acetone until no identifiable green needle tissue remained. A small amount of sand, $MgCO_3$ and ascorbic acid were added to help with grinding and to prevent acidification and pigment degradation. The extracts were then centrifuged and diluted. Using a spectrophotometer (Go Direct SpectroVis Plus Spectrophotometer; Vernier), the absorbance of the supernatant was measured at 470, 645, 662 and 710 nm. Pigment pools were calculated on a leaf area basis including chlorophyll a ($Chla_{area}$), chlorophyll b ($Chlb_{area}$) and bulk carotenoids (Car_{area}; ug/cm^2 for all pools) were calculated according to Lichtenthaler (1987). The total chlorophyll pool size (Chl_{area} = $Chla_{area}$ + $Chlb_{area}$) and ratios Chla:$Chlb_{area}$ and Chl:Car_{area} were also calculated.

2.7 | Spectral reflectance

Needle spectral reflectance was measured with a spectroradiometer (UniSpec SC; PP Systems) with an attached fibre optic probe (UNI400; PP Systems) and specialized needle clip (UNI501; PP Systems). The spectroradiometer allowed sampling of the spectrum between 310 and 1100 nm with a 3.3 nm sampling interval which was afterwards reduced to 1 nm using linear interpolation. After collecting dark and white standard (Spectralon; LabSphere) reference measurements, three spectral measurements were made on each branch to capture spatial heterogeneity. Reflectance values were calculated from the spectral measurements by dividing each foliage measurement by the measurement from the white standard. The photochemical reflectance index (PRI) was calculated according to the equation: (R531 − R570)/(R531 + R570) (Gamon et al., 1992; Penuelas et al., 1995) where R531 and R570 are the reflectances at 531 and 570 nm, respectively.

2.8 | Statistical analyses

Relationships between measured foliar parameters (physiology, pigments and leaf traits), and integrated daily PPFD and location (BRF or the FTE) were assessed using linear mixed effects models. The interaction between PPFD and location was included so as to examine the variations in slope between locations. Individual tree (FTE n = 18, BRF n = 6) was included as a random effect to account for repeat measures on trees [Parameter ~ PPFD × location + (1 | tree)]. If necessary, parameters were log-transformed to meet assumptions of normality of the residuals. Parameter estimates were considered significantly different from zero if $p < 0.05$. Linear mixed effects analysis was conducted using the lme4 package (Bates et al., 2015) with the lmerTest package loaded to provide p values (Kuznetsova et al., 2017). All analyses took place in R v. 4.1.0 (R Core Team, 2022).

The effects of canopy position and location on foliar traits were also assessed using mixed effects models implemented in the lme4 package (Bates et al., 2015). Again, individual tree was included as a random effect to account for repeat measures on trees. Pairwise comparisons between canopy position (high or low) and location (FTE or BRF) were assessed using the emmeans package in R and found to be significant if $p < 0.05$ (Lenth, 2020). All data reported below are means ± SE. Finally, the relationships between physiological parameters and either N_{area} or total chlorophyll ($Chl + Car_{area}$) were also examined using linear mixed effects models. A description of the full models can be found in the Supporting Information: Methods S1.

3 | RESULTS

3.1 | Tree characteristics and growth environment

Tree characteristics for the trees measured in this study have been previously reported in Griffin et al. (2022) but have been summarized in Table 1. Briefly, trees from BRF tended to have a larger DBH (measured at 1.37 m from the ground) with BRF trees having an average diameter of 23.1 ± 1.99 cm and FTE trees having an average diameter of 16.7 ± 0.94 cm (Table 1). Trees from the two locations were also extremely different in their average dripline areas (27.34 ± 2.00 m^2 at BRF vs. 3.52 ± 0.37 m^2 at the FTE; Table 1). Nevertheless, despite these differences trees from the two locations had very similar average heights (9.91 ± 0.73 m at BRF and 9.32 ± 0.57 m at the FTE; Table 1).

Irradiance at the range extremes of white spruce, from the northernmost location at the FTE in Alaska, to the southernmost location at BRF in New York, showed pronounced differences in both intensity and day length (Figure 1a–d). Average ambient PPFD over the measurement campaigns (Figure 1a; orange) estimated from daily diurnal light courses modelled from canopy photos (e.g., 4 July 2017; Figure 1b) was 36% higher at BRF than at the FTE (54.4 ± 0.03 compared to 39.9 ± 0.06 mol m^{-2} day^{-1}). However, day length was much longer at the FTE than at BRF (Figure 1b). At the canopy positions where physiological and biochemical measurements were made, average daily PPFD was significantly greater at high canopy positions than low canopy positions at both BRF and the FTE (34.97 ± 0.16 vs. 9.20 ± 0.13 mol m^{-2} day^{-1} at BRF, and 29.24 ± 0.16 vs. 21.14 ± 0.16 mol m^{-2} day^{-1} at the FTE; Figure 1a). Even so, the difference in the daily mean PPFD experienced from the upper to the lower canopies was much smaller at the FTE than at BRF (only 8 mol m^{-2} day^{-1} at the FTE vs. 25 mol m^{-2} day^{-1} at BRF). This narrowing of the irradiance gradient across vertical canopy positions

13653040, 2023, 1, Downloaded from https://onlinelibrary.wiley.com/doi/10.1111/pce.14448 by Columbia University Libraries, Wiley Online Library on [05/09/2024]. See the Terms and Conditions (https://onlinelibrary.wiley.com/terms-and-conditions) on Wiley Online Library for rules of use; OA articles are governed by the applicable Creative Commons License

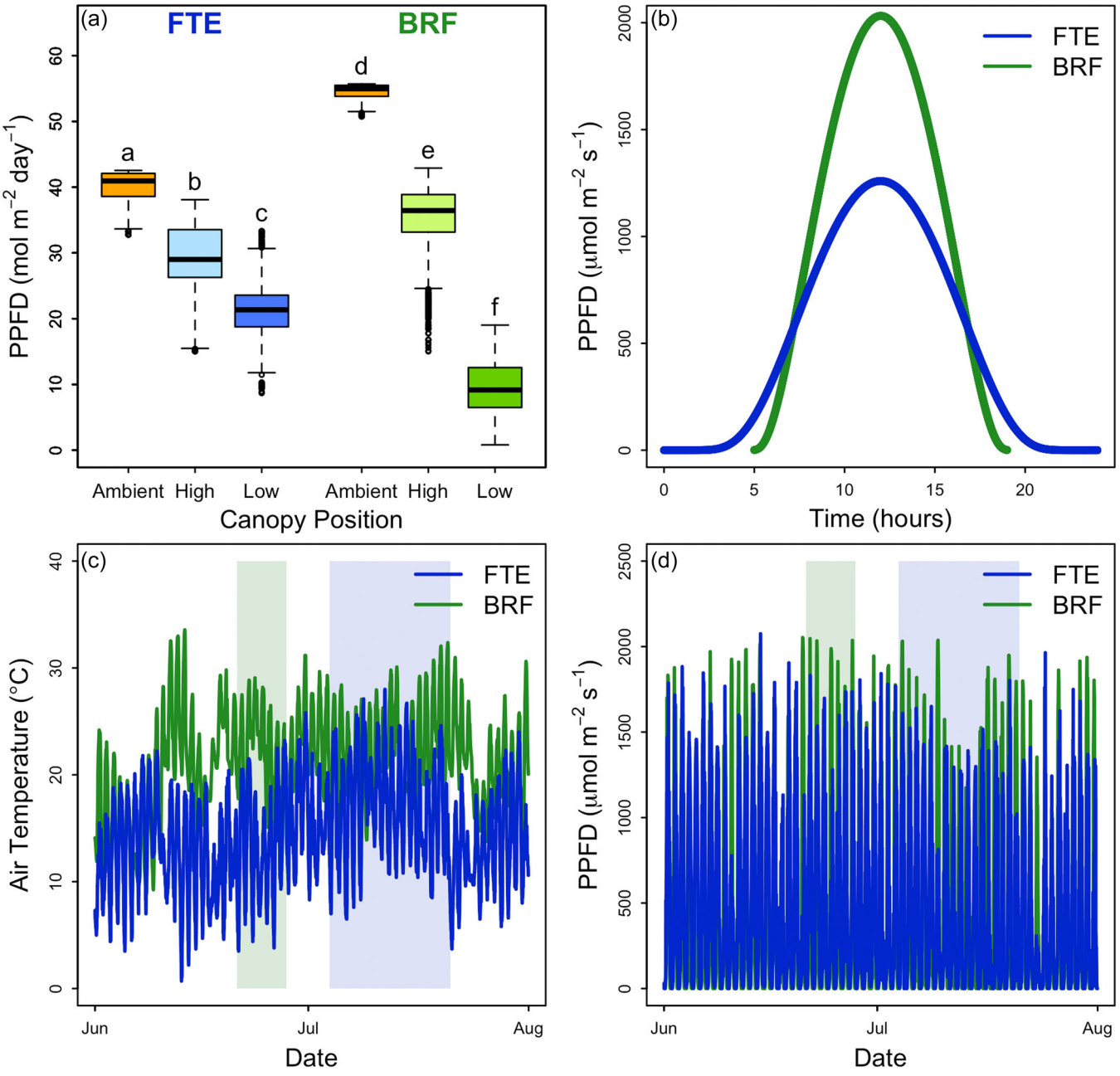


FIGURE 1 (a) Average daily PPFD calculated from canopy photos over the study period (June to July) at the FTE, Alaska and BRF, New York. Ambient (above canopy) PPFD is shown in orange. Boxplots show the median and first and third quartiles. Whiskers display the range of groups with individual points representing outliers falling outside 1.5 times the interquartile range. Different letters represent significant differences between locations and canopy positions ($p < 0.05$). (b) Ambient PPFD projected from canopy photos during 1 day (4 July 2017) at both locations. (c) Air temperature (°C) measured at BRF and the FTE for June and July 2017. (d) Ambient PPFD measured from field instruments at BRF and the FTE for June and July 2017. Green and blue shaded areas in 1c and 1d denote the dates of the study campaigns at BRF and the FTE, respectively. BRF, Black Rock Forest; FTE, forest tundra ecotone; PPFD, photosynthetic photon flux density.

at the FTE was decoupled from canopy height, given that trees at both locations were of similar heights.

In addition to differences in the light environment, there were also pronounced differences in the daytime air temperatures between the two locations (Figure 1c). During the respective study campaigns (as marked by the green (BRF) and blue (FTE) shaded areas (Figure 1c)), BRF mean daytime temperature was 23.4°C, with a minimum temperature of 12.8°C and a maximum temperature of 29.1°C, whereas the FTE mean temperature was 17°C, with a minimum temperature of 6.5°C and a maximum temperature of 28°C. Thus, the FTE experienced colder temperatures and greater temperature variability.

13653040, 2023, 1, Downloaded from https://onlinelibrary.wiley.com/doi/10.1111/pce.14448 by Columbia University Libraries, Wiley Online Library on [05/09/2024]. See the Terms and Conditions (https://onlinelibrary.wiley.com/terms-and-conditions) on Wiley Online Library for rules of use; OA articles are governed by the applicable Creative Commons License

3.2 | Relationships between light environment and gas exchange, biochemistry, pigments and PRI

In general, significant relationships were found between average PPFD and physiological traits, biochemical traits, pigment concentrations and PRI at BRF. In contrast, few significant relationships were found between average PPFD and foliar traits at the FTE (Table 2).

3.2.1 | Photosynthesis and respiration

A significant positive relationship was observed between average PPFD and A_{1500} at BRF with high canopy foliage having a higher A_{1500} than low canopy foliage. No significant relationship was observed between A_{1500} and average PPFD at the FTE, nor were there any significant differences between the canopy positions (Figure 2a, Table 2, Supporting Information: S1 & S2). Across all samples at each location, mean A_{1500} was found to be 40% higher at BRF than at the FTE (10.8 ± 0.5 at BRF vs. 7.7 ± 0.4 μmol m^{-2} s^{-1} at the FTE; Supporting Information: Table S2). The differences between BRF and the FTE in the relationship of A_{1500} to PPFD correspond to differences in several other parameters commonly extracted from light response curves. Namely the following were observed at BRF: a significant negative relationship between average PPFD and Φ (Figure 2b, Table 2), with significantly lower Φ in the high than the low canopy (Figure 2b, Supporting Information: Tables S1 & S2); and significant positive relationships between average PPFD and LSP, LCP, R_D and R_L with higher values in the high than the low canopies (Figures 2c–f, Table 2, Supporting Information: S1 & S2). At the FTE, as in the case of A_{1500}, no significant relationship was found between average PPFD and Φ, LCP, R_D or R_L (Figures 2b–f, Table 2); however, a significant positive relationship was found between average PPFD and LSP with a correspondingly higher LSP in the high canopy than the low canopy foliage at both locations (Figure 2c, Table 2, Supporting Information: S1 & S2). Across all samples at each location, Φ was significantly lower at the FTE than at BRF (0.03 ± 0.001 at the FTE vs. 0.05 ± 0.002 at BRF; Supporting Information: Tables S1 & S2), and LSP, LCP, R_D and R_L were significantly higher at the FTE than at BRF [LSP = 644 ± 14 at the FTE vs. 522 ± 18.6 μmol m^{-2} s^{-1} at BRF; LCP = 90.7 ± 4.5 at the FTE vs. 36.8 ± 2.1 μmol m^{-2} s^{-1} at BRF (LCP means are backtransformed); R_D = 2.46 ± 0.11 at the FTE vs. 1.98 ± 0.14 μmol m^{-2} s^{-1} at BRF; R_L = 2.22 ± 0.12 at the FTE vs. 1.58 ± 0.16 μmol m^{-2} s^{-1} at BRF; Supporting Information: Tables S1 & S2]. In particular, the differences in mean R_L between the two locations were dramatic, with the FTE having 41% higher R_L than at BRF.

The parameters extracted from the A-C_i curves (V_{cmax} and J_{max} normalized to 25°C) also followed the positive relationship between PPFD and A_{1500} at BRF. Both V_{cmax} and J_{max} had positive relationships with PPFD and significantly higher values in the high than the low canopy at BRF (Figure 3, Table 2, Supporting Information: S1 & S2). However, the expected lack of a relationship with PPFD at the FTE was not observed. Instead, FTE V_{cmax} and J_{max} both had significant negative relationships with PPFD, with significantly lower values in the high than the low canopy. Consequently, when values from canopy positions were pooled to compare the two locations, no significant differences were observed between the FTE and BRF (V_{cmax} = 48.5 ± 1.7 at the FTE and 50.3 ± 2.2 μmol m^{-2} s^{-1} at BRF; J_{max} = 80.8 ± 2.7 at the FTE and 85.9 ± 3.4 μmol m^{-2} s^{-1} at BRF; Supporting Information: Tables S1 & S2).

3.2.2 | Leaf traits

A significant negative relationship was observed between SLA and PPFD at BRF while no relationship was observed between SLA and PPFD at the FTE (Figure 4a, Table 2). Across canopy positions, high canopy foliage had significantly lower SLA at both locations (Figure 4a, Supporting Information: Tables S1 & S2). The FTE had significantly lower SLA than BRF (32.0 ± 1.1 at the FTE vs. 50.4 ± 1.2 $cm^2 g^{-1}$ at BRF, Supporting Information: Tables S1 & S2). %N showed no significant relationships with PPFD, and no significant differences between canopy positions in either location; although the FTE did have a small but significantly lower %N than BRF (0.98 ± 0.03 at the FTE vs. 1.1 ± 0.04 at BRF; Figure 4c, Table 2, Supporting Information: S1 & S2). Similarly, C:N showed no significant relationships with PPFD and no significant differences between canopy positions in either location; however, C:N was significantly lower at BRF compared to the FTE (Table 2, Supporting Information: S1 & S2). Due to the strong relationship between SLA and PPFD, N_{area} also had a significant positive relationship with PPFD at BRF and no relationship at the FTE (Figure 4e, Table 2).

3.2.3 | Pigments and spectral indices

With regard to pigment concentrations, positive relationships were seen both at BRF and the FTE in the ratio of chlorophyll a and chlorophyll b (Chla:$Chlb_{area}$) and in the Carotenoids (Car_{area}) with higher Chla:$Chlb_{area}$ and higher Car_{area} in the high than the low canopies (Figure 4b,d, Table 2, Supporting Information: S1 & S2). The expected decrease in the ratio of chlorophyll to carotenoids (Chl:Car_{area}) with increasing PPFD was observed at BRF, but no relationship was found at the FTE (Figure 2f, Table 2). However, the FTE did have 46% more carotenoids than BRF (14.5 ± 0.5 at the FTE vs. 9.9 ± 0.8 μg cm^{-2} at BRF; Supporting Information: Tables S1 & S2) and a significantly lower Chl:Car_{area} (6.7 ± 0.2 at the FTE vs. 9.0 ± 0.3 at BRF; Supporting Information: Tables S1 & S2). Finally, PRI had the expected positive relationship with Chl:Car_{area} at BRF (Figure 5, Table 3, Supporting Information: S3) and it decreased significantly with increasing PPFD at BRF (Figure 5, Table 2). However, no relationships between PRI and Chl:Car_{area} or PPFD were found at the FTE (Figure 5, Tables 2 and 3, Supporting Information: S3).

13653040, 2023, 1, Downloaded from https://onlinelibrary.wiley.com/doi/10.1111/pce.14448 by Columbia University Libraries, Wiley Online Library on [05/09/2024]. See the Terms and Conditions (https://onlinelibrary.wiley.com/terms-and-conditions) on Wiley Online Library for rules of use; OA articles are governed by the applicable Creative Commons License

TABLE 2 Parameter estimates for the linear mixed effects models in which each physiological, leaf and spectral trait was modelled as a function of integrated average daily photochemical photon flux density (PPFD) and location [either Black Rock Forest (BRF), New York, or the forest tundra ecotone (FTE), Alaska] with a random effect for each individual tree [Parameter ~ PPFD × location + (1 | tree)]

	Intercepts		Slopes			
Parameter	**BRF**	**FTE**	**BRF**	**FTE**	r_m^2	r_c^2
Photosynthesis						
A_{1500}	**9.282 (0.730)***a**	**9.542 (1.389)***a**	**0.066 (0.024)**a**	−0.075 (0.054)$^{+}$b	0.4	0.5
Φ	**0.055 (0.003)***a**	**0.039 (0.004)***b**	**−2e−04 (1e−04)**a**	−3e−04 (2e−04)$^{+}$a	0.67	0.82
LSP	**366.132 (29.038)***a**	**540.489 (51.805)***b**	**6.912 (0.855)***a**	**4.185 (2.012)*a**	0.57	0.69
log(LCP)	**2.744 (0.116)***a**	**4.170 (0.223)***b**	**0.038 (0.004)***a**	0.014 (0.009)b	0.75	0.79
V_{cmax}	**43.123 (3.494)***a**	**68.472 (6.867)***b**	**0.316 (0.112)**a**	**−0.796 (0.270)**b**	0.17	0.31
J_{max}	**73.760 (5.499)***a**	**108.241 (10.866)***b**	**0.531 (0.178)**a**	**−1.092 (0.427)*b**	0.17	0.31
Respiration						
R_D	**0.72 (0.211)**a**	**2.321 (0.411)***b**	**0.055 (0.007)***a**	0.006 (0.016)b	0.48	0.58
R_L	0.299 (0.228)a	**1.726 (0.403)***b**	**0.055 (0.007)***a**	0.020 (0.016)b	0.52	0.62
Leaf traits						
% Carbon	**47.498 (0.514)***a**	**49.003 (0.630)***a**	**0.020 (0.007)**a**	−0.015 (0.023)a	0.08	0.8
% Nitrogen	**1.064 (0.052)***a**	**0.972 (0.095)***a**	0.002 (0.001)a	4e−04 (0.004)a	0.17	0.53
C_{area}	**702.603 (58.824)***a**	**1481.729 (139.897)***b**	**13.332 (2.136)***a**	2.254 (5.484)a	0.71	0.71
N_{area}	**15.084 (1.684)***a**	**26.773 (2.842)***b**	**0.349 (0.037)***a**	0.176 (0.109)a	0.58	0.81
log(C:N)	**3.822 (0.053)***a**	**3.9303 (0.100)***a**	−0.002 (0.001)a	−9e−04 (0.004)a	0.18	0.54
SLA	**65.803 (2.053)***a**	**34.393 (4.748)***b**	**−0.676 (0.072)***a**	−0.089 (0.186)b	0.76	0.77
Pigments						
Chl_{area}	**77.180 (5.705)***a**	**89.363 (11.060)***a**	0.325 (0.178)$^{+}$a	0.288 (0.407)a	0.21	0.44
$Chla_{area}$	**48.129 (3.576)***a**	**54.266 (6.907)***a**	**0.304 (0.111)*a**	0.367 (0.254)a	0.3	0.51
$Chlb_{area}$	**29.06 (2.353)***a**	**35.186 (4.55)***a**	0.021 (0.073)a	−0.082 (0.167)a	0.09	0.36
Car_{area}	**6.058 (0.905)***a**	**10.722 (1.795)***b**	**0.170 (0.030)***a**	**0.160 (0.066)*a**	0.67	0.74
$Chl:Car_{area}$	**11.583 (0.461)***a**	**7.973 (0.901)***b**	**−0.116 (0.015)***a**	−0.052 (0.033)a	0.69	0.77
$Chla:Chlb_{area}$	**1.673 (0.070)***a**	**1.510 (0.128)***a**	**0.009 (0.002)***a**	**0.017 (0.005)***a**	0.35	0.63

13653040, 2023, 1, Downloaded from https://onlinelibrary.wiley.com/doi/10.1111/pce.14448 by Columbia University Libraries, Wiley Online Library on [05/09/2024]. See the Terms and Conditions (https://onlinelibrary.wiley.com/terms-and-conditions) on Wiley Online Library for rules of use; OA articles are governed by the applicable Creative Commons License

TABLE 2 (Continued)

Parameter	Intercepts		Slopes		r_m^2	r_c^2
	BRF	FTE	BRF	FTE		
Spectral indices						
PRI	**0.051 (0.006)***a**	0.005 (0.015)b	**−9e−04 (2e−04)***a**	8e−04 (6e−04)b	0.24	0.31

Note: Values in parentheses are SEs. Bolded and starred values are those that are significantly different from zero (***$p < 0.001$; **$p < 0.01$; **$p < 0.05$; +$p < 0.1$). Significant differences between locations are indicated by different letters ($p < 0.05$). Marginal and conditional coefficients of determination (r_m^2 and r_c^2, respectively) are also reported.

Abbreviations: A_{1500}, photosynthesis at 1500 μmol $m^{-2}s^{-1}$; Φ, apparent quantum yield; C_{area}, carbon per leaf area (mg C cm^{-2}); Car_{area}, area-based carotenoid content (μg cm^{-2}); Chl_{area}, total chlorophyll on an area basis (μg cm^{-2}); $Chla_{area}$, area-based chlorophyll a content (μg cm^{-2}); $Chlb_{area}$, area-based chlorophyll b content (μg cm^{-2}); Chl:Car_{area}, ratio of total chlorophyll content to carotenoids; Chla:$Chlb_{area}$, ratio of chlorophyll a to chlorophyll b; C:N, carbon to nitrogen ratio; J_{max}, maximum electron transport (μmol $m^{-2}s^{-1}$); LCP, light compensation point (μmol $m^{-2}s^{-1}$); LSP, light saturation point (μmol $m^{-2}s^{-1}$); N_{area}, nitrogen per leaf area (mg N cm^{-2}); PRI, photochemical reflectance index; R_D, respiration in the dark (μmol $m^{-2}s^{-1}$); R_L, respiration in the light (μmol $m^{-2}s^{-1}$); SLA, specific leaf area (cm^2g^{-1}); V_{cmax}, maximum carboxylation rate (μmol $m^{-2}s^{-1}$).

3.2.4 | Relationships between gas exchange traits and nitrogen

As with PPFD, positive relationships were found between N_{area} and A_{1500}, and N_{area} and V_{cmax} at BRF while no relationships were observed at the FTE (Figure 6a,b, Table 3, Supporting Information: S3). In contrast, both BRF and the FTE had positive relationships between N_{area} and R_D (Figure 6c, Table 3, Supporting Information: S3), between N_{area} and R_L (Table 3, Supporting Information: S3) and between N_{area} and total pigments (chla+ chlb+ carotenoids; Figure 6d, Table 3, Supporting Information: S3).

3.3 | Carbon balance at the range extremes of white spruce

The collection of gas exchange parameters such as V_{cmax} and J_{max}, which are commonly used to predict photosynthesis, together with values of respiration at 25°C (R_{25}) previously reported by Griffin et al. (2022), provide a unique opportunity to examine the carbon balance across the range extremes of white spruce. We find that, when all parameters are normalized to 25°C, the ratios of V_{cmax} and J_{max} to R_{25} are 228% higher at BRF than at the FTE (Figure 7, Supporting Information: Tables S1 & S2; $V_{cmax}/R_{25} = 21.4 \pm 1.39$ at the FTE vs. 70.2 ± 7.47 at BRF; $J_{max}/R_{25} = 36.5 \pm 2.45$ at the FTE vs. 119.9 ± 13.21 at BRF). No significant differences were observed in the ratios between canopy positions at each location, although there was a trend for larger ratios in the low canopy than the high canopy at BRF (Figure 7, Supporting Information: Tables S1 & S2).

4 | DISCUSSION

4.1 | Local environmental conditions drive differences in tree structure between white spruce range extremes

Vertical canopy gradients of foliar physiological and biochemical traits differ between white spruce growing at its northern- and southern-most range limits. Whereas steep canopy gradients in physiological functioning are found at the southern range limit in BRF, a clear lack of variation in foliar physiological capacity is observed between the high and low canopies of white spruce at its northernmost range extreme in the FTE. As our two study locations delimit the distributional range of white spruce and are separated by a distance of more than 5000 km, these differences are likely in response to local environmental conditions. Solar zenith angles, day length, air and soil temperatures, soil moisture and vapour pressure deficit vary substantially between these two locations. Of these environmental conditions, the impacts of local light environment are of particular interest for the following reasons: (1) light energy is a critical driver of photosynthetic carbon gain (Hirose & Werger, 1987); (2) abundant evidence shows that canopy gradients in photosynthetic

13653040, 2023, 1, Downloaded from https://onlinelibrary.wiley.com/doi/10.1111/pce.14448 by Columbia University Libraries, Wiley Online Library on [05/09/2024]. See the Terms and Conditions (https://onlinelibrary.wiley.com/terms-and-conditions) on Wiley Online Library for rules of use; OA articles are governed by the applicable Creative Commons License

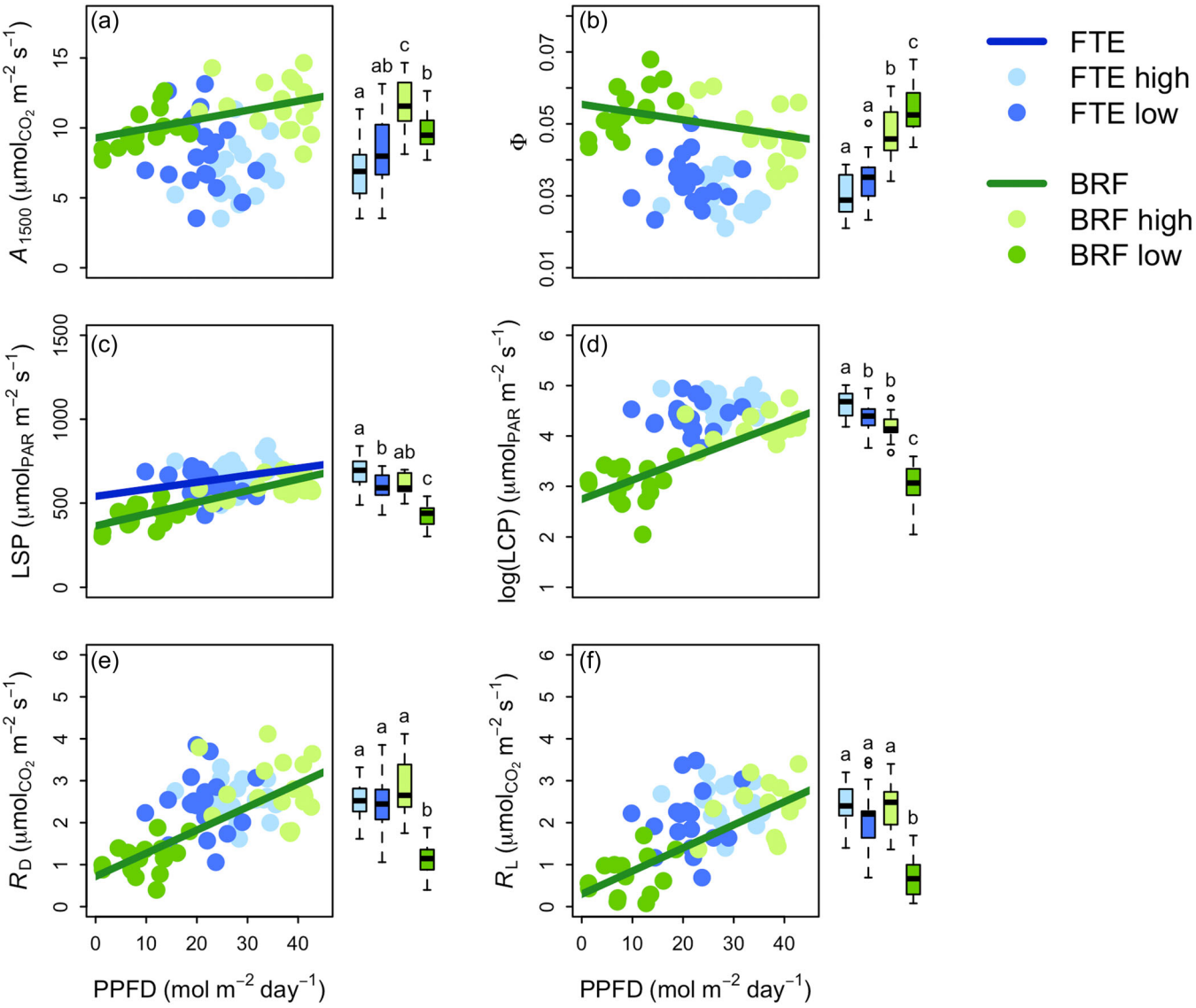


FIGURE 2 Linear relationships between average daily photosynthetic photon flux density (PPFD) over the measurement campaign and area-based foliar photosynthetic characteristics of white spruce from the FTE (blue), Alaska and BRF (green), New York including photosynthesis at 1500 µmol $m^{-2}s^{-1}$ (A_{1500}; 2a; FTE $n = 38$; BRF $n = 33$), apparent quantum yield (Φ; 2b; FTE $n = 38$; BRF $n = 33$), light saturation point (LSP; 2c; FTE $n = 38$; BRF $n = 33$), light compensation point (LCP; 2d; FTE $n = 38$; BRF $n = 33$), respiration in the dark (R_D; 2e; FTE $n = 38$; BRF $n = 36$) and respiration in the light (R_L; 2f; FTE $n = 37$; BRF $n = 29$). Light and dark colours at each location (BRF or FTE) represent high and low canopy positions, respectively. Parameter estimates of the linear mixed effects regression models, and statistical differences between slopes and intercepts are presented in Table 2. Regression lines are only shown for significant relationships (slope $p < 0.05$). Furthermore, included are boxplots by canopy position and location for each parameter. Different letters represent significant differences between locations and canopy positions ($p < 0.05$; Supporting Information: Tables S1 & S2). BRF, Black Rock Forest; FTE, forest tundra ecotone. [Color figure can be viewed at wileyonlinelibrary.com]

traits are strongly correlated to gradients in irradiance throughout tree crowns (Bond et al., 1999; Ellsworth & Reich, 1993; Field, 1983; Hirose & Werger, 1987; Niinemets et al., 2015), but little work assesses the impacts of latitudinal location on these gradients within a single species; and (3) these gradients are key parameters in ecosystem models used to calculate gross primary productivity (GPP) across latitudinal space (Bonan et al., 2012; Rogers et al., 2017). Day length and solar zenith angles increase and light intensity decreases as one moves towards the northernmost latitudes of the globe (Nilsen, 1983; Slaughter & Viereck, 1986). These local light environments are further modified by differences in forest and tree crown structure between the two locations. Trees at the southern location exist within a complex forest canopy comprised of deciduous hardwood species where they must compete for light energy and other above-ground resources. Consequently white spruce tree crowns are distinctly conical in shape with a wide dripline area in the southern location, presumably to minimize self-shading and maximize light energy capture. In contrast, trees at the northern

13653040, 2023, 1, Downloaded from https://onlinelibrary.wiley.com/doi/10.1111/pce.14448 by Columbia University Libraries, Wiley Online Library on [05/09/2024]. See the Terms and Conditions (https://onlinelibrary.wiley.com/terms-and-conditions) on Wiley Online Library for rules of use; OA articles are governed by the applicable Creative Commons License

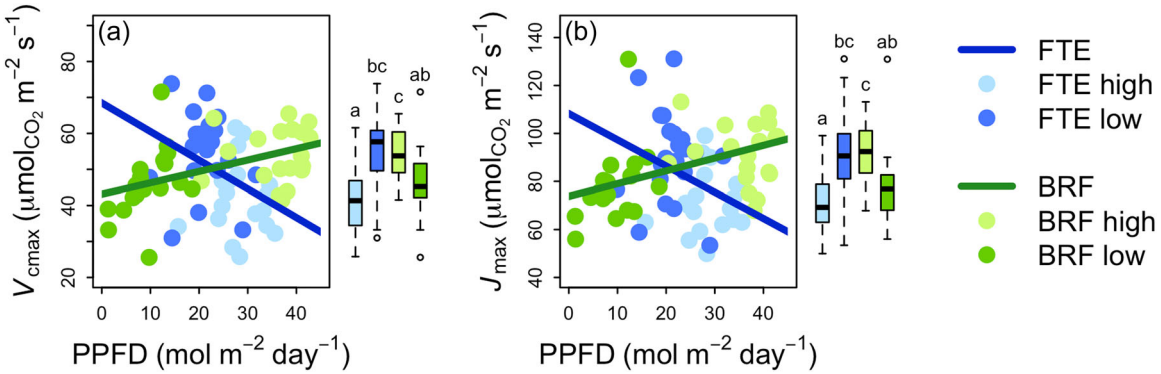


FIGURE 3 Linear relationships between average daily photosynthetic photon flux density (PPFD) and foliar respiratory characteristics on an area basis of white spruce from the FTE (blue), Alaska and BRF (green), New York including the maximum rate of carboxylation (V_{cmax}; 3a; FTE $n = 39$; BRF $n = 37$), and the maximum electron transport rate (J_{max}; 3b; FTE $n = 39$; BRF $n = 37$). Light and dark colours at each location (BRF or FTE) represent high and low canopy positions, respectively. Parameter estimates of the linear mixed effects regression models, and statistical differences between slopes and intercepts are presented in Table 2. Regression lines are only shown for significant relationships (slope $p < 0.05$). Furthermore, included are boxplots by canopy position and location for each respiratory parameter. Different letters represent significant differences between locations and canopy positions ($p < 0.05$; Supporting Information: Tables S1 & S2). BRF, Black Rock Forest; FTE, forest tundra ecotone. [Color figure can be viewed at wileyonlinelibrary.com]

location are widely spaced with narrow and untapering tree crowns. The open forest canopy minimizes competition for resources such as light. Furthermore, the cylindrical shape promotes more equal exposure of foliage to irradiance in a region of the globe with extremely high solar zenith angles, ultimately increasing the efficiency of light capture for photosynthesis (Kuuluvainen, 1992). Overall, these solar and structural differences lead to a narrowing of the intracanopy light gradients as one moves from the southern (where light availability is ~35 and ~9 mol m^{-2} day^{-1} at the high and low canopies, respectively) to the northern (where light availability is ~29 and ~21 mol m^{-2} day^{-1} at the high and low canopies, respectively) latitudinal limits of this species.

4.2 | Vertical gradients in physiological function are coordinated to latitudinal differences in light environment

Inherent to the structural differences of trees in these two locations is the need for tree crowns to organize their physiological and biochemical traits to optimize photosynthetic carbon gain (Hirose & Werger, 1987; Niinemets et al., 1998). Therefore, at BRF, where there are strong intracanopy light gradients, we find strongly positive relationships between PPFD and A_{1500}, J_{max} and V_{cmax} indicating the upregulation of the light reactions (in which RuBP is produced) and the carbon reactions (in which rubisco acts on RuBP to fix carbon) of photosynthesis in the high canopy (Givnish, 1988; Valladares & Niinemets, 2008). The elevated metabolic activity in the high canopy results in higher respiratory activity to support the costs of growth and protein maintenance (Griffin et al., 2001; Lewis et al., 2000; Reich et al., 1998). Biochemical traits also follow the inherent light gradients. High light needles have lower SLA and a greater N_{area} reflecting the greater leaf thickness of high light leaves from added palisade layers and the presence of nitrogen in both the enzyme rubisco and in chlorophyll (Evans, 1989; Evans & Poorter, 2001; Smith et al., 1997). Finally, high light leaves have greater Car_{area} and a smaller Chl:Car_{area} ratio reflecting the need for greater photoprotection from excess light energy (Demmig-Adams & Adams, 1992). In all cases, biochemical and physiological traits of low latitude white spruce conform to the established literature showing strong correlations with canopy gradients of irradiance. At the high latitude location where intracanopy light gradients become less pronounced, we see the absence of canopy gradients in many physiological and biochemical traits. What is most striking is the lack of relationships between irradiance and each of photosynthesis (A_{1500}), light respiration, and dark respiration. Together with the lack of relationships between irradiance and the apparent quantum yield, the light compensation point, SLA and N_{area}, these findings suggest that the uneven distribution of metabolic activity throughout the canopy required to optimize photosynthetic carbon gain in correspondence with canopy irradiance gradients at low latitudes does not occur at high latitudes where irradiance varies minimally throughout the canopy profile.

The parameters discussed above suggest that northern latitude trees have few distinguishable canopy gradients in photosynthetic physiology. However, positive relationships between irradiance and the ratio of Chla to Chlb, the light saturation point and carotenoid concentrations suggest that even though the magnitude of the light gradient narrows at northern latitudes, there is still a subtle intracanopy light gradient to which pigments are responding. Thus, in the higher light upper canopy we see greater investments in Chla than Chlb to maximize light capture and a greater investment in carotenoids to dissipate excess light energy and protect photosynthetic machinery (Dale & Causton, 1992; Hikosaka & Terashima, 1995; Kitajima & Hogan, 2003; Magney et al., 2016; Ruban, 2015; Scartazza et al., 2016). It is possible that these subtle canopy

13653040, 2023, 1, Downloaded from https://onlinelibrary.wiley.com/doi/10.1111/pce.14448 by Columbia University Libraries, Wiley Online Library on [05/09/2024]. See the Terms and Conditions (https://onlinelibrary.wiley.com/terms-and-conditions) on Wiley Online Library for rules of use; OA articles are governed by the applicable Creative Commons License

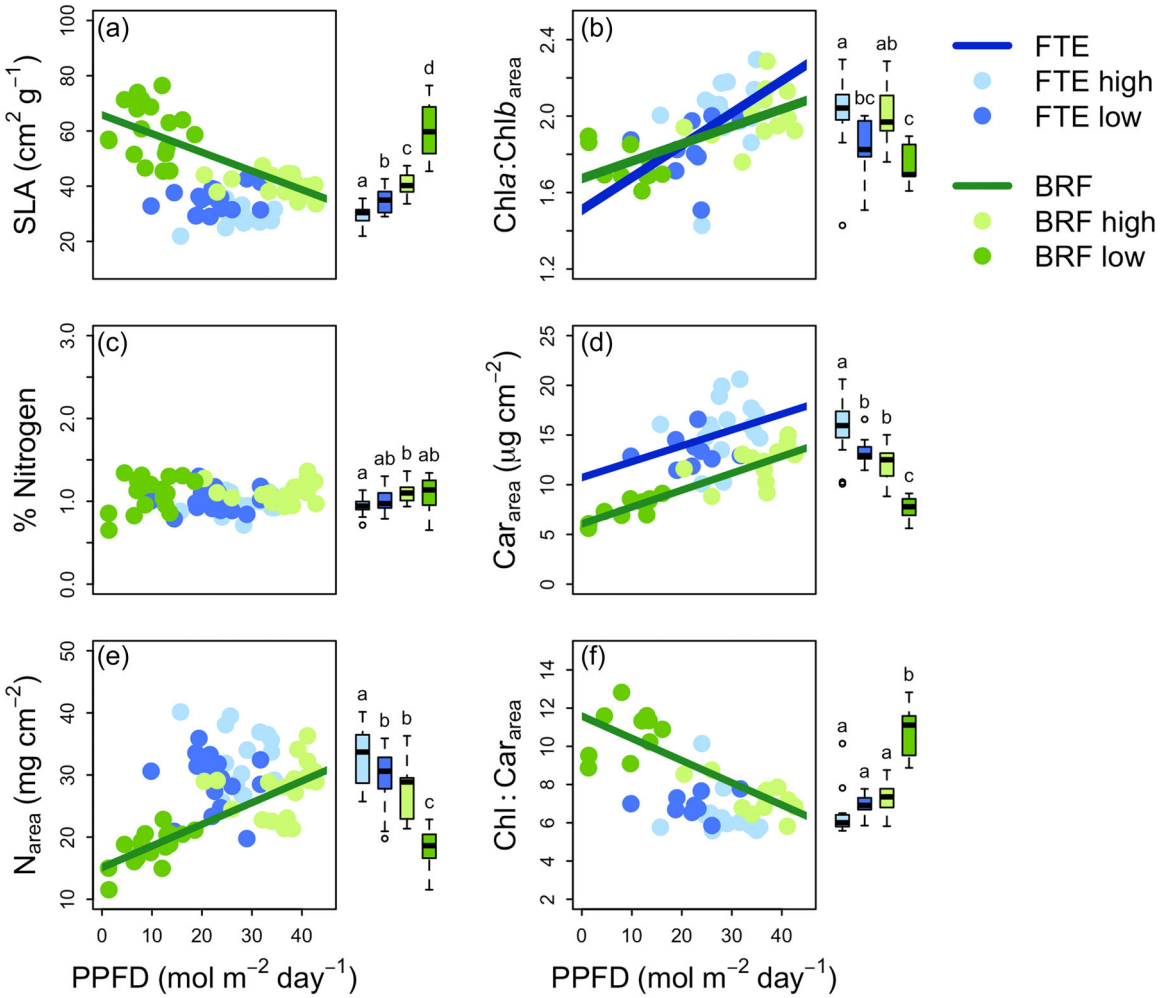


FIGURE 4 Linear relationships between average daily photosynthetic photon flux density (PPFD) and leaf traits of white spruce from the FTE (blue), Alaska and BRF (green), New York including specific leaf area (SLA; 4a; FTE $n = 37$; BRF $n = 38$), the ratio of chlorophyll a to chlorophyll b (Chla:Chlb$_{area}$; 4b; FTE $n = 25$; BRF $n = 22$), % nitrogen (4c; FTE $n = 37$; BRF $n = 38$), carotenoids (Car$_{area}$; 4d; FTE $n = 25$; BRF $n = 22$), nitrogen per leaf area (N$_{area}$; 4e; FTE $n = 37$; BRF $n = 38$) and the ratio of chlorophylls a+ b to carotenoids (Chl:Car$_{area}$; 4c; FTE $n = 25$; BRF $n = 22$). Light and dark colours at each location (BRF or FTE) represent high and low canopy positions, respectively. Parameter estimates of the linear mixed effects models, and statistical differences between slopes and intercepts are presented in Table 2. Regression lines are only shown for significant relationships (slope $p < 0.05$). Furthermore, included are boxplots by canopy position and location for each leaf trait. Different letters represent significant differences between locations and canopy positions ($p < 0.05$; Supporting Information: Tables S1 & S2). BRF, Black Rock Forest; FTE, forest tundra ecotone. [Color figure can be viewed at wileyonlinelibrary.com]

gradients in pigments may be a result of the 24 h of light exposure during the growing season at the FTE.

In contrast to the lack of relationships found between irradiance and the majority of traits, and the subtle positive relationships found between irradiance and pigments at treeline, we find a surprising downregulation of J_{max} and V_{cmax} in the high canopy foliage at the FTE. It is unclear why we find these negative relationships between irradiance and the component processes of photosynthesis at the northern locations; however, there are several possible explanations and hypotheses that could be further explored. One possibility is that the combination of diminutive vertical canopy gradients in light, SLA and nitrogen, the latter of which is critical to the performance of J_{max} and V_{cmax} because of the presence of nitrogen in chlorophyll and the enzyme rubisco (Evans, 1989; Evans & Poorter, 2001; Smith et al., 1997), has led to the observed negative relationships. However, strong relationships do exist between nitrogen and total pigment concentrations even though there is no apparent relationship between nitrogen and V_{cmax}. Furthermore, we still find weak positive relationships between irradiance and both carotenoid concentrations and Chla:Chlb even with a narrow light gradient. Consequently, we conclude that a more mechanistic explanation must exist for the puzzling downregulation of V_{cmax} and J_{max}. While in this study we focused on the latitudinal relationships between canopy light environments and foliar physiological traits, it is possible that intracanopy gradients in other environmental conditions may also impact V_{cmax} and J_{max} measurements (Bachofen et al., 2020; Bauerle et al., 2009; Buckley, 2021; Martin et al., 1999; Zweifel et al., 2002). Perhaps of particular relevance with respect to rubisco carboxylation

13653040, 2023, 1, Downloaded from https://onlinelibrary.wiley.com/doi/10.1111/pce.14448 by Columbia University Libraries, Wiley Online Library on [05/09/2024]. See the Terms and Conditions (https://onlinelibrary.wiley.com/terms-and-conditions) on Wiley Online Library for rules of use; OA articles are governed by the applicable Creative Commons License

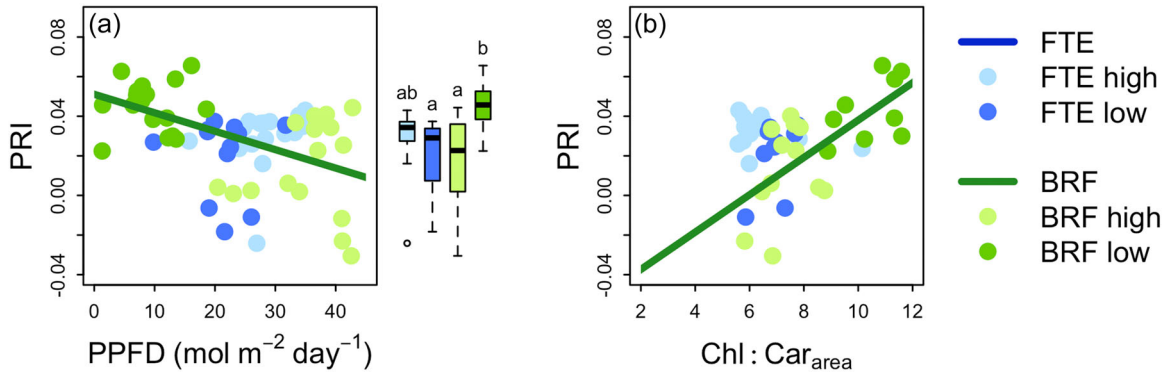


FIGURE 5 Linear relationships between photochemical reflectance index (PRI) and either average daily photosynthetic photon flux density (PPFD) (5a; FTE $n = 30$; BRF $n = 34$) or the ratio of chlorophylls a+ b to carotenoids (Chl:Car$_{area}$; 5b) of white spruce from the FTE (blue), Alaska and BRF (green), New York. Light and dark colours at each location (BRF or FTE) represent high and low canopy positions, respectively. Parameter estimates of the linear mixed effects regression models, and statistical differences between slopes and intercepts are presented in Table 2. Regression lines are only shown for significant relationships (slope $p < 0.05$). Furthermore, included are boxplots by canopy position and location for PRI. Different letters represent significant differences between locations and canopy positions ($p < 0.05$; Supporting Information: Tables S1 & S2). BRF, Black Rock Forest; FTE, forest tundra ecotone. [Color figure can be viewed at wileyonlinelibrary.com]

TABLE 3 Parameter estimates for the intercepts and slopes of linear mixed effects models with tree as a random effect examining relationships between photosynthesis at 1500 µmol m^{-2}s^{-1} (A_{1500}), maximum rate of carboxylation (V_{cmax}), respiration in the dark (R_D), respiration in the light (R_L) or total pigment content (Chl + Car$_{area}$) and nitrogen per leaf area (N$_{area}$); as well as the relationship between photochemical reflectance index (PRI) and the chlorophyll to carotenoid ratio (Chl:Car$_{area}$)

Model	Intercepts BRF	FTE	Slopes BRF	FTE	r_m^2	r_c^2
A_{1500}~ N$_{area}$ × location	**6.181 (1.250)***a**	**8.130 (2.220)***a**	**0.200 (0.049)***a**	−0.024 (0.071)b	0.5	0.64
V_{cmax} ~ N$_{area}$ × location	**28.828 (6.253)***a**	**61.318 (12.106)***b**	**0.934 (0.230)***a**	−0.440 (0.383)b	0.15	0.55
R_D ~ N$_{area}$ × location	−0.761 (0.410)$^+$a	0.714 (0.620)a	**0.118 (0.017)***a**	**0.055 (0.020)**b**	0.49	0.49
R_L ~ N$_{area}$ × location	−0.908 (0.518)$^+$a	0.386 (0.723)a	**0.113 (0.021)***a**	**0.059 (0.023)*a**	0.42	0.42
(Chl + Car$_{area}$) ~ N$_{area}$ × location	**62.309 (11.765)***a**	**63.348 (22.613)**a**	**1.436 (0.501)**a**	**1.518 (0.712)*a**	0.39	0.52
PRI ~ Chl:Car$_{area}$ × location	**−0.060 (0.015)***a**	0.033 (0.023)b	**0.010 (0.002)***a**	−0.0008 (0.003)b	0.43	0.54

Note: In all models tree was included as a random effect. Values in parentheses are SEs. Bolded and starred values are those that are significantly different from zero (***$p < 0.001$; **$p < 0.01$; *$p < 0.05$; +$p < 0.1$). Significant differences between locations are indicated by different letters ($p < 0.05$). Marginal and conditional coefficients of determination (r_m^2 and r_c^2 respectively) are also reported.

Abbreviations: BRF, Black Rock Forest; FTE, forest tundra ecotone.

is the reliance of this process on the enzyme rubisco, whose activity is well-known to be temperature dependent (Benomar et al., 2018; Yamori & von Caemmerer, 2009). Work at alpine treelines has clearly documented that as trees grow in stature, their foliage becomes increasingly coupled to atmospheric conditions such as temperature and wind stress (Körner, 2012). These stresses may be detrimental to high canopy photosynthetic performance (lowering V_{cmax} and J_{max}). In contrast, low canopy foliage is less coupled to atmospheric conditions and may therefore be more protected from temperature and wind extremes (Germino & Smith, 1999; Johnson et al., 2004; Maguire et al., 2019; Martin et al., 1999).

Temperature and wind stress are not the only environmental conditions likely to cause reduced gradients in physiological functioning. Hydraulic conductance has also been found to vary in response to water availability, impacting canopy gradients in nitrogen and photosynthesis (Peltoniemi et al., 2012). It is equally possible that winter temperature extremes may impact hydraulic function in exposed foliage. Consequently, throughout the canopy of Alaskan trees there may be a constant balancing act with regard to the resource allocation necessary to improve whole canopy photosynthetic carbon gain. Two factors compete with each other: namely the need to devote resources to light capture in the high canopy where irradiance is slightly more available; and the need to devote resources either to foliage protection in the high canopy or increased carbon gain in the low canopy when harsh conditions prevail. The result, ultimately, is what we find across the majority of physiological and biochemical traits, that is, a lack of variation in photosynthetic carbon gain across the high and low canopy in high latitude trees. Without detailed information on temperature, wind and hydraulic profiles throughout the canopy, this hypothesis cannot be fully

13653040, 2023, 1, Downloaded from https://onlinelibrary.wiley.com/doi/10.1111/pce.14448 by Columbia University Libraries, Wiley Online Library on [05/09/2024]. See the Terms and Conditions (https://onlinelibrary.wiley.com/terms-and-conditions) on Wiley Online Library for rules of use; OA articles are governed by the applicable Creative Commons License

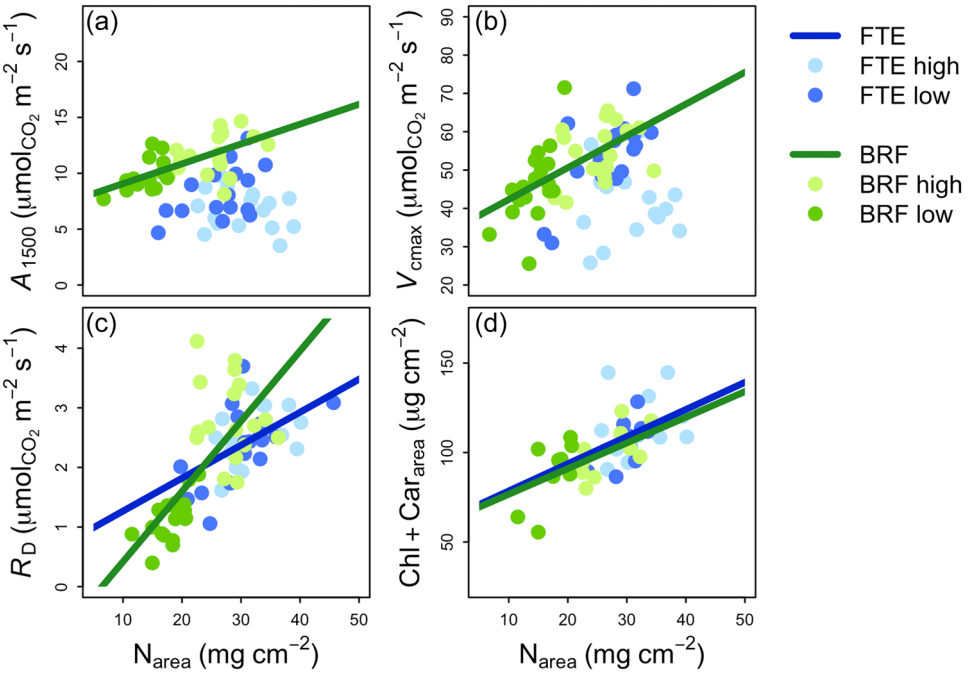


FIGURE 6 Linear relationships between photosynthesis at 1500 µmol $m^{-2}s^{-1}$ (A_{1500}; 6a), maximum rate of carboxylation (V_{cmax}; 6b), respiration in the dark (R_D; 6c) and total pigment content (Chl + Car_{area}; 6d) versus nitrogen per leaf area (N_{area}) of white spruce from the FTE (blue), Alaska and BRF (green), New York. Light and dark colours at each location (BRF or FTE) represent high and low canopy positions, respectively. Parameter estimates of the linear mixed effects regression models, and statistical differences between slopes and intercepts are presented in Table 3 & Supporting Information: Table S3. Regression lines are only shown for significant relationships (slope $p < 0.05$). BRF, Black Rock Forest; FTE, forest tundra ecotone. [Color figure can be viewed at wileyonlinelibrary.com]

tested. Yet, it seems clear from the linkages between irradiance, photosynthesis and tree structure across the latitudinal extremes that the environment is an integral driver of species' geographic range. We suggest that expanding to examine additional environmental conditions such as temperature, wind and water stress may be a compelling future direction, thereby adding to our overall understanding of the mechanisms controlling canopy carbon exchange across the massive FTE and more broadly across latitudinal gradients.

The accurate portrayal of canopy gradients is important to the precise prediction of carbon exchange and GPP (Bonan et al., 2012; Sands, 1995). However, the lack of variation in photosynthesis at the FTE suggests that complex canopy models used to account for canopy self-shading at mid-latitudes may not be necessary to model GPP in trees from high latitudes. The lack of variation in PRI across vertical canopy positions at the FTE similarly suggests that accounting for canopy self-shading may be less critical at northern latitudes as opposed to mid-latitudes. PRI has previously been demonstrated to be an accurate predictor of whole canopy GPP in broad-leaved species when used in concert with terrestrial Light Detection and Ranging (LiDAR) to account for canopy self-shading (Coops et al., 2017; Hilker et al., 2008). Although our own study does not employ LiDAR, the presence of canopy differences in PRI at the southernmost location suggests that such a technique could work equally well in mid-latitude coniferous forests. Furthermore, the fact that PRI mirrors A_{1500} regardless of latitude suggests that this remotely sensed index may be a valuable future tool for accurately assessing GPP of other species with different structural properties and with large latitudinal distributions.

4.3 | Physiological and biochemical traits may contribute to the range limits of white spruce

The detailed data on the physiology and biochemistry of white spruce not only allow for the examination of canopy differences across latitudinal range extremes, but also for the examination of locational differences in traits that may further illuminate possible drivers contributing to the range limits of this important species. Here, we observed important differences in physical and biochemical traits such as SLA, % N, C:N and carotenoid concentration between the southern and northern range extremes. Most relevant to the above discussion of light environment and its impacts on photosynthetic physiology is the finding of significantly higher carotenoid concentrations in needles of northern white spruce compared to southern white spruce. This indicates a greater investment in photoprotection at northern latitudes during the growing season. Elevated carotenoids at the northern range extreme may be in response to the 24 h photoperiod at the Arctic tundra boreal forest ecotone. Past studies have found that very high levels of light protecting xanthophyll pigments can be a feature of Arctic plants subjected to continuous light (Magney et al., 2019). Lower overall SLA in Alaskan needles compared to BRF needles indicates that foliage at the northern edge

13653040, 2023, 1, Downloaded from https://onlinelibrary.wiley.com/doi/10.1111/pce.14448 by Columbia University Libraries, Wiley Online Library on [05/09/2024]. See the Terms and Conditions (https://onlinelibrary.wiley.com/terms-and-conditions) on Wiley Online Library for rules of use; OA articles are governed by the applicable Creative Commons License

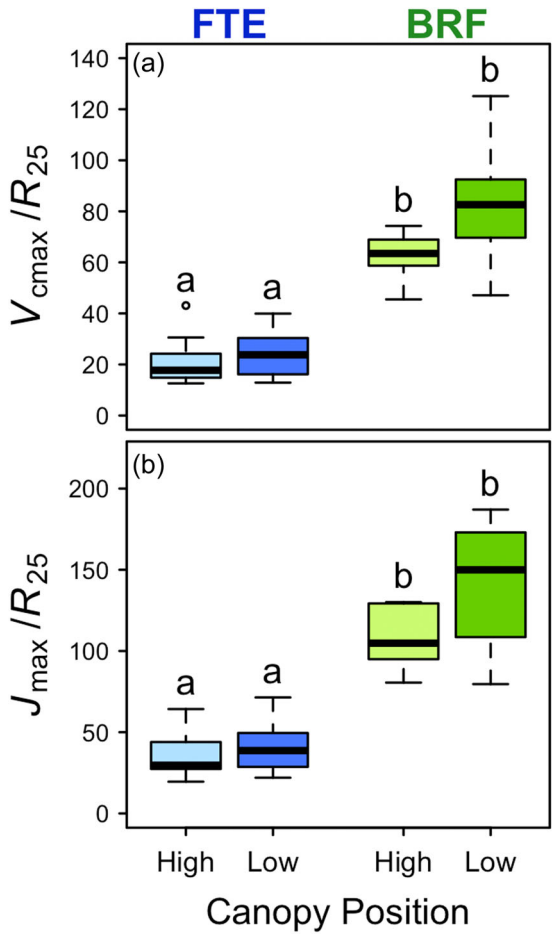


FIGURE 7 Ratios of (a) maximum rate of carboxylation to respiration at 25°C from Griffin et al. (2022) (V_{cmax}/R_{25}) and (b) maximum electron transport rate to respiration at 25°C from Griffin et al. (2022) (J_{max}/R_{25}) of white spruce from high and low canopy positions at the FTE (blue), Alaska and BRF (green), New York. Boxplots show the median and first and third quartiles. Whiskers display the range of groups with individual points representing outliers falling outside 1.5 times the interquartile range. Different letters represent significant differences between locations and canopy positions ($p < 0.05$; Supporting Information: Tables S1 & S2). BRF, Black Rock Forest; FTE, forest tundra ecotone. [Color figure can be viewed at wileyonlinelibrary.com]

of the distribution is thicker or denser. Although decreasing SLA is commonly found in response to increasing light availability due to the added density of additional photosynthetic machinery (as seen throughout the BRF canopy), SLA is also commonly positively correlated to ambient growth temperatures (Atkin et al., 2006; Poorter et al., 2009). Thus, a low SLA at the FTE may indicate a greater investment in needle structure rather than photosynthetic machinery, a hypothesis that is corroborated by our finding of higher carbon to nitrogen ratios in Alaskan needles (González-Zurdo et al., 2016). Investment in structure is potentially adaptive in the harsh FTE where needles must survive multiple years of winter temperatures, snow or ice accumulation and windblown ice abrasion. Leaf nitrogen was also found to be slightly but significantly lower in needles from the northern range limit. This result confirms the findings of Griffin et al. (2022) and agrees with past studies that show negative correlations between nitrogen and both temperature and latitude (Körner, 1989; Reich & Oleksyn, 2004; Yin, 1993). Nitrogen biogeochemistry is intimately linked to environmental and ecological factors. For example, harsh temperatures and unique hydrologic and permafrost dynamics inherent to the Arctic can slow decomposition rates and depress nitrogen fixation (Schimel et al., 2004; Schimel & Stuart Chapin, 1996). The result is the limited availability of nitrogen in the harsh northern latitudes of the globe. The differences in biochemical and structural traits between our two study locations hint at environmental drivers, in addition to light availability, that should be considered in future studies examining latitudinal differences in canopy gradients.

Finally, in addition to biochemical differences between locations, metabolic differences are key in understanding the mechanisms controlling the range limits of this species. Previous work in white spruce shows this species to have extremely high rates of dark respiration at its northern compared to southern range limit, a finding that has led to the conclusion that respiratory carbon loss may be a crucial factor constraining the northern range limit of this species (Griffin et al., 2022). We find similar patterns in the current study, with significantly higher rates of dark respiration (as estimated from the light response curves) in white spruce in Alaska than in New York. Furthermore, we find that these differences are apparent not only in the dark respiration, but also in light respiration. Given that the northern range extreme of this species experiences 24 h of sunlight during the majority of the growing season, the greater rates of light respiration in FTE compared to BRF trees provides important corroboration of the constancy of the extreme respiratory cost at this northern range limit and the role it may play in determining the location of northern treeline. It is likely that these high respiratory fluxes to the atmosphere are related to high maintenance costs given the harsh environmental conditions of the region.

Northern white spruce are not only characterized by high carbon losses. The additional information on photosynthetic processes provided here further suggests that these carbon costs are not matched by similarly high carbon gains. We do not directly compare the ratios of photosynthetic carbon gain to respiratory carbon loss due to the use of different measurement temperatures chosen to reflect ambient conditions in each location, but the ability to normalize both V_{cmax} and J_{max} to 25°C allows us to assess the carbon balance of white spruce at its latitudinal range extremes. The results of this comparison are dramatic and demonstrate that northern trees function within a much narrower margin to maintain a positive carbon balance. It seems that it is not only high respiratory costs that result in slow growth rates of white spruce and constrain the latitudinal range limit of northern treeline. Instead, our study suggests that it is the combined effect of high respiration and low V_{cmax} and J_{max} that ultimately limit the northern range of this widely distributed and important boreal species.

13653040, 2023, 1, Downloaded from https://onlinelibrary.wiley.com/doi/10.1111/pce.14448 by Columbia University Libraries, Wiley Online Library on [05/09/2024]. See the Terms and Conditions (https://onlinelibrary.wiley.com/terms-and-conditions) on Wiley Online Library for rules of use; OA articles are governed by the applicable Creative Commons License

5 | CONCLUSIONS

White spruce spans a massive distribution, the extremes of which are characterized by vastly different environmental conditions. Here we demonstrate that differences in local light environment correlate to differences in vertical canopy physiology, resource allocation and crown structure. Thus, at high latitudes where light intensity is low, solar zenith angles are high and day length is long, there is a clear lack of variation between high and low canopy white spruce traits. In contrast, white spruce at lower latitudes exist in a complex forest canopy of deciduous hardwood species and experience greater differences in local and canopy light environments leading to steep gradients in physiological and biochemical traits between high and low canopy positions. Consequently, accounting for self-shading may be less critical for predicting GPP at northern relative to southern latitudes. Our findings point to light environment as an important driver in latitudinal variation in physiology within a single species and emphasize the importance of the connection between environment and physiology in determining a species' distributional range. Furthermore, our findings highlight that additional environmental drivers such as temperature, and water availability may also contribute both to canopy and latitudinal differences in physiological traits.

These data not only allowed us to examine the role of physiology in determining a species' distributional range, but they also permitted us to question the role of a species' carbon balance in determining the extreme limit of tree growth form. Previous work has highlighted that extreme respiratory costs may be a critical component leading to the latitudinal location of northern treeline. Here we demonstrate that it is not only extreme respiratory costs but also minimal photosynthetic carbon gains that together may determine the latitudinal location of the world's largest ecotone and the transition from boreal forest to treeless tundra.

ACKNOWLEDGEMENTS

We thank Sarah Sacket from the NASA ABoVE support team in Fairbanks, A. K., for her energetic and prompt logistical support during Alaska field campaigns. At Black Rock Forest, we also wish to acknowledge the unflagging support of BRF staff including Ben Brady and Matthew Munson as well as Dr. William Schuster, the Executive Director of Black Rock. This study was supported by NASA ABoVE grant NNX15AT86A, the Arctic LTER (NSF Grant No. 1637459 & 2220863) and the Plant Resilience Institute at Michigan State University.

DATA AVAILABILITY STATEMENT

The data in this study are archived in the ORNL DAAC as: Schmiege, S.C., K. Griffin, N. Boelman, L. Vierling, S.G. Bruner, E. Min, A.J. Maguire, J. Jensen, J. Eitel (2022) White Spruce Photosynthetic, Leaf, Pigment and Spectral Traits, AK and NY, US, 2017. ORNL DAAC, Oak Ridge, Tennessee, USA. https://doi.org/10.3334/ORNLDAAC/2124.

ORCID

Stephanie C. Schmiege https://orcid.org/0000-0001-9054-5538
Kevin L. Griffin http://orcid.org/0000-0003-4124-3757
Natalie T. Boelman https://orcid.org/0000-0003-3716-2372
Sarah G. Bruner https://orcid.org/0000-0001-7103-9664
Elizabeth Min https://orcid.org/0000-0001-7889-6693
Andrew J. Maguire http://orcid.org/0000-0002-6334-0497
Johanna Jensen https://orcid.org/0000-0001-8811-7091

REFERENCES

Akalusi M.E., Meng F.R. & Bourque C.P.-A. (2021) Photosynthetic parameters and stomatal conductance in attached and detached balsam fir foliage. *Plant-Environment Interactions*, 2, 206–215.

Arguez A., Durre I., Applequist S., Vose R.S., Squires M.F., Yin X. et al. (2012) NOAA's 1981–2010 US climate normals: an overview. *Bulletin of the American Meteorological Society*, 93, 1687–1697.

Atkin O.K., Loveys B.R., Atkinson L.J. & Pons T.L. (2006) Phenotypic plasticity and growth temperature: understanding interspecific variability. *Journal of Experimental Botany*, 57, 267–281.

Ayub G., Smith R.A., Tissue D.T. & Atkin O.K. (2011) Impacts of drought on leaf respiration in darkness and light in *Eucalyptus saligna* exposed to industrial-age atmospheric CO_2 and growth temperature. *New Phytologist*, 190, 1003–1018.

Bachofen C., D'Odorico P. & Buchmann N. (2020) Light and VPD gradients drive foliar nitrogen partitioning and photosynthesis in the canopy of European beech and silver fir. *Oecologia*, 192, 323–339.

Bates D., Maechler M., Bolker B. & Walker S. (2015) Fitting linear mixed-effects models using lme4. *Journal of Statistical Software*, 67, 1–48.

Bauerle W.L., Bowden J.D., Wang G.G. & Shahba M.A. (2009) Exploring the importance of within-canopy spatial temperature variation on transpiration predictions. *Journal of Experimental Botany*, 60, 3665–3676.

Benomar L., Lamhamedi M.S., Pepin S., Rainville A., Lambert M.-C., Margolis H.A. et al. (2018) Thermal acclimation of photosynthesis and respiration of southern and northern white spruce seed sources tested along a regional climatic gradient indicates limited potential to cope with temperature warming. *Annals of Botany*, 121, 443–457.

Bolker B. & R Development Core Team. (2020) bbmle: tools for general maximum likelihood estimation. R package version 1.0.23.1. https://CRAN.R-project.org/package=bbmle

Bonan G.B., Oleson K.W., Fisher R.A., Lasslop G. & Reichstein M. (2012) Reconciling leaf physiological traits and canopy flux data: use of the TRY and FLUXNET databases in the Community Land Model version 4. *Journal of Geophysical Research: Biogeosciences*, 117, 1–19.

Bond B.J., Farnsworth B.T., Coulombe R.A. & Winner W.E. (1999) Foliage physiology and biochemistry in response to light gradients in conifers with varying shade tolerance. *Oecologia*, 120, 183–192.

Brown J.H., Stevens G.C. & Kaufmnan D.M. (1996) The geographic range: size, shape, boundaries, and internal structure. *Annual Review of Ecology and Systematics*, 27, 597–623.

Buckley T.N. (2021) Optimal carbon partitioning helps reconcile the apparent divergence between optimal and observed canopy profiles of photosynthetic capacity. *New Phytologist*, 230, 2246–2260.

Buckley T.N., Vice H. & Adams M.A. (2017) The Kok effect in *Vicia faba* cannot be explained solely by changes in chloroplastic CO_2 concentration. *New Phytologist*, 216, 1064–1071.

Coops N.C., Hermosilla T., Hilker T. & Black T.A. (2017) Linking stand architecture with canopy reflectance to estimate vertical patterns of light-use efficiency. *Remote Sensing of Environment*, 194, 322–330.

Dale M.P. & Causton D.R. (1992) Use of the chlorophyll a/b ratio as a bioassay for the light environment of a plant. *Functional Ecology*, 6, 190–196.

13653040, 2023, 1, Downloaded from https://onlinelibrary.wiley.com/doi/10.1111/pce.14448 by Columbia University Libraries, Wiley Online Library on [05/09/2024]. See the Terms and Conditions (https://onlinelibrary.wiley.com/terms-and-conditions) on Wiley Online Library for rules of use; OA articles are governed by the applicable Creative Commons License

Demmig-Adams, B. & Adams, W.W., III (1992) Photoprotection and other responses of plants to high light stress. *Annual Review of Plant Physiology and Plant Molecular Biology*, 43, 599–626.

Duursma R.A. (2015) Plantecophys—an R package for analysing and modelling leaf gas exchange data. *PLoS One*, 10, e0143346.

Eitel J.U.H., Griffin K.L., Boelman N.T., Maguire A.J., Meddens A.J.H., Jensen J. et al. (2020) Foliar remote sensing tracks radial tree growth dynamics. *Global Change Biology*, 26, 4068–4078.

Eitel J.U.H., Maguire A.J., Boelman N., Vierling L.A., Griffin K.L., Jensen J. et al. (2019) Proximal remote sensing of tree physiology at northern treeline: do late-season changes in the photochemical reflectance index (PRI) respond to climate or photoperiod? *Remote Sensing of Environment*, 221, 340–350.

Ellsworth D.S. & Reich P.B. (1993) Canopy structure and vertical patterns of photosynthesis and related leaf traits in a deciduous forest. *Oecologia*, 96, 169–178.

Evans J.R. (1989) Photosynthesis and nitrogen relationships in leaves of C_3 plants. *Oecologia*, 78, 9–19.

Evans J.R. & Poorter H. (2001) Photosynthetic acclimation of plants to growth irradiance: the relative importance of specific leaf area and nitrogen partitioning in maximizing carbon gain. *Plant, Cell and Environment*, 24, 755–767.

Farquhar G.D. & Busch F.A. (2017) Changes in the chloroplastic CO_2 concentration explain much of the observed Kok effect: a model. *New Phytologist*, 214, 570–584.

Farquhar G.D., von Caemmerer S. & Berry J.A. (1980) A biochemical model of photosynthetic CO_2 assimilation in leaves of C_3 species. *Planta*, 149, 78–90.

Field C. (1983) Allocating leaf nitrogen for the maximization of carbon gain: leaf age as a control on the allocation program. *Oecologia*, 56, 341–347.

Gamon A., Penuelas J. & Field C.B. (1992) A narrow-waveband spectral index that tracks diurnal changes in photosynthetic efficiency. *Remote Sensing of Environment*, 41, 35–44.

Gamon J.A., Huemmrich K.F., Wong C.Y., Ensminger I., Garrity S., Hollinger D.Y. et al. (2016) A remotely sensed pigment index reveals photosynthetic phenology in evergreen conifers. *Proceedings of the National Academy of Sciences USA*, 113, 13087–13092.

Gaston K.J. (1996) Species-range-size distributions: patterns, mechanisms and implications. *Trends in Ecology and Evolution*, 11, 197–201.

Germino M.J. & Smith W.K. (1999) Sky exposure, crown architecture, and low-temperature photoinhibition in conifer seedlings at alpine treeline. *Plant, Cell and Environment*, 22, 407–415.

Givnish T.J. (1988) Adaptation to sun and shade: a whole-plant perspective. *Australian Journal of Plant Physiology*, 15, 63–92.

González-Zurdo P., Escudero A., Babiano J., García-Ciudad A. & Mediavilla S. (2016) Costs of leaf reinforcement in response to winter cold in evergreen species. *Tree Physiology*, 36, 273–286.

Griffin K.L., Griffin Z.M., Schmiege S.C., Bruner S., Boelman N.T., Vierling L.A. et al. (2022) Variation in white spruce needle respiration at the species range limits: a potential impediment to northern expansion. *Plant, Cell & Environment*, 45, 1–15.

Griffin K.L., Schmiege S.C., Bruner S.G., Boelman N.T., Vierling L.A. & Eitel J.U.H. (2021) High leaf respiration rates may limit the success of white spruce saplings growing in the kampfzone at the Arctic treeline. *Frontiers in Plant Science*, 12, 746464.

Griffin K.L., Tissue D.T., Turnbull M.H., Schuster W. & Whitehead D. (2001) Leaf dark respiration as a function of canopy position in *Nothofagus fusca* trees grown at ambient and elevated CO_2 partial pressures for 5 years. *Functional Ecology*, 15, 497–505.

Harley P.C. & Baldocchi D.D. (1995) Scaling carbon dioxide and water vapour exchange from leaf to canopy in a deciduous forest. I. Leaf model parametrization. *Plant, Cell and Environment*, 18, 1146–1156.

Herrmann H.A., Schwartz J.M. & Johnson G.N. (2020) From empirical to theoretical models of light response curves—linking photosynthetic and metabolic acclimation. *Photosynthesis Research*, 145, 5–14.

Heskel M.A., Atkin O.K., Turnbull M.H. & Griffin K.L. (2013) Bringing the Kok effect to light: a review on the integration of daytime respiration and net ecosystem exchange. *Ecosphere*, 4, 1–14.

Hikosaka K. & Terashima I. (1995) A model of the acclimation of photosynthesis in the leaves of C_3 plants to sun and shade with respect to nitrogen use. *Plant, Cell and Environment*, 18, 605–618.

Hilker T., Coops N.C., Schwalm C.R., Jassal R.S., Black T.A. & Krishnan P. (2008) Effects of mutual shading of tree crowns on prediction of photosynthetic light-use efficiency in a coastal Douglas-fir forest. *Tree Physiology*, 28, 825–834.

Hirose T. & Werger M.J.A. (1987) Maximizing daily canopy photosynthesis with respect to the leaf nitrogen allocation pattern in the canopy. *Oecologia*, 72, 520–526.

Johnson D.M., Germino M.J. & Smith W.K. (2004) Abiotic factors limiting photosynthesis in *Abies lasiocarpa* and *Picea engelmannii* seedlings below and above the alpine timberline. *Tree Physiology*, 24, 377–386.

Kirschbaum M.U. & Farquhar G.D. (1987) Investigation of the CO_2 dependence of quantum yield and respiration in *Eucalyptus pauciflora*. *Plant Physiology*, 83, 1032–1036.

Kitajima K. & Hogan K.P. (2003) Increases of chlorophyll a/b ratios during acclimation of tropical woody seedlings to nitrogen limitation and high light. *Plant, Cell and Environment*, 26, 857–865.

Kok B. (1948) A critical consideration of the quantum yield of *Chlorella*-photosynthesis. *Enzymologia*, 13, 1–56.

Körner C. (1989) The nutritional status of plants from high altitudes—a worldwide comparison. *Oecologia*, 81, 379–391.

Körner C. (2012) *Alpine treelines: functional ecology of the global high elevation tree limits*. Springer.

Kuuluvainen T. (1992) Tree architectures adapted to efficient light utilization: is there a basis for latitudinal gradients? *Nordic Society Oikos*, 65, 275–284.

Kuznetsova A., Brockhoff P. & Christensen R. (2017) Lmertest package: tests in linear mixed effects models. *Journal of Statistical Software*, 82, 1–26.

Lambers H. & Oliveira R.S. (2019) Physiological ecology and the distribution of organisms, *Plant physiological ecology*. Springer, pp. 2–5.

Lenth R. (2020) *Emmeans: estimated marginal means, aka least-squares means. R package version 1.4.5*. https://CRAN.R-project.org/package=emmeans

Lewis J.D., McKane R.B., Tingey D.T. & Beedlow P. A. (2000) Vertical gradients in photosynthetic light response within an old-growth Douglas-fir and western hemlock canopy. *Tree Physiology*, 20, 447–456.

Lichtenthaler H.K. (1987) Chlorophylls and carotenoids: pigments of photosynthetic biomembranes. *Methods in Enzymology*, 148, 350–382.

Lowry E. & Lester S.E. (2006) The biogeography of plant reproduction: potential determinants of species' range sizes. *Journal of Biogeography*, 33, 1975–1982.

Magney T.S., Bowling D.R., Logan B.A., Grossmann K., Stutz J., Blanken P.D. et al. (2019) Mechanistic evidence for tracking the seasonality of photosynthesis with solar-induced fluorescence. *Proceedings of the National Academy of Sciences of the United States of America*, 116, 11640–11645.

Magney T.S., Eitel J.U.H., Griffin K.L., Boelman N.T., Greaves H.E., Prager C.M. et al. (2016) LiDAR canopy radiation model reveals patterns of photosynthetic partitioning in an Arctic shrub. *Agricultural and Forest Meteorology*, 221, 78–93.

Maguire A.J., Eitel J.U.H., Vierling L.A., Johnson D.M., Griffin K.L., Boelman N.T. et al. (2019) Terrestrial lidar scanning reveals fine-scale linkages between microstructure and photosynthetic

13653040, 2023, 1, Downloaded from https://onlinelibrary.wiley.com/doi/10.1111/pce.14448 by Columbia University Libraries, Wiley Online Library on [05/09/2024]. See the Terms and Conditions (https://onlinelibrary.wiley.com/terms-and-conditions) on Wiley Online Library for rules of use; OA articles are governed by the applicable Creative Commons License

functioning of small-stature spruce trees at the forest-tundra ecotone. *Agricultural and Forest Meteorology*, 269–270, 157–168.
Martin T.A., Hinckley T.M., Meinzer F.C. & Sprugel D.G. (1999) Boundary layer conductance, leaf temperature and transpiration of *Abies amabilis* branches. *Tree Physiology*, 19, 435–443.
Mavi, H.S. & Tupper, G.J. (2004) Solar radiation and its role in plant growth, *Agrometeorology: principles and applications of climate studies in agriculture*. Food Products Press, pp. 13–42.
Niinemets Ü. (2007) Photosynthesis and resource distribution through plant canopies. *Plant, Cell & Environment*, 30, 1052–1071.
Niinemets Ü., Keenan T.F. & Hallik L. (2015) A worldwide analysis of within-canopy variations in leaf structural, chemical and physiological traits across plant functional types. *New Phytologist*, 205, 973–993.
Niinemets U., Kull O. & Tenhunen J.D. (1998) An analysis of light effects on foliar morphology, physiology and light interception in temperate deciduous woody species of contrasting shade tolerance. *Tree Physiology*, 18, 681–696.
Nilsen J. (1983) Light climate in northern areas. In: Kaurin A., Junttila O. & Nilsen J. (Eds.) *Plant production in the north*. Norwegian University Press, pp. 62–72.
Patterson A.E., Arkebauer R., Quallo C., Heskel M.A., Li X., Boelman N. et al. (2018) Temperature response of respiration and respiratory quotients of 16 co-occurring temperate tree species. *Tree Physiology,*, 38, 1319–1332.
Peltoniemi M.S., Duursma R.A. & Medlyn B.E. (2012) Co-optimal distribution of leaf nitrogen and hydraulic conductance in plant canopies. *Tree Physiology*, 32, 510–519.
Penuelas J., Filella I. & Gamon J.A. (1995) Assessment of photosynthetic radiation-use efficiency with spectral reflectance. *New Phytologist*, 131, 291–296.
Poorter H., Niinemets Ü., Poorter L., Wright I.J. & Villar R. (2009) Causes and consequences of variation in leaf mass per area (LMA): a meta-analysis. *New Phytologist*, 182, 565–588.
de Pury D.G.G. & Farquhar G.D. (1997) Simple scaling of photosynthesis from leaves to canopies without the errors of big-leaf models. *Plant, Cell and Environment*, 20, 537–557.
R Core Team. (2022) R: a language and environment for statistical computing. R Foundation for Statistical Computing. Vienna, Austria. https://www.R-project.org/
Reich P.B. & Oleksyn J. (2004) Global patterns of plant leaf N and P in relation to temperature and latitude. *Proceedings of the National Academy of Sciences of the United States of America*, 101, 11001–11006.
Reich P.B., Walters M.B., Ellsworth D.S., Vose J.M., Volin J.C., Gresham C. et al. (1998) Relationships of leaf dark respiration to leaf nitrogen, specific leaf area and leaf life-span: a test across biomes and functional groups. *Oecologia*, 114, 471–482.
Rogers A., Medlyn B.E., Dukes J.S., Bonan G., von Caemmerer S., Dietze M.C. et al. (2017) A roadmap for improving the representation of photosynthesis in earth system models. *New Phytologist*, 213, 22–42.
Ruban A.V. (2015) Evolution under the sun: optimizing light harvesting in photosynthesis. *Journal of Experimental Botany*, 66, 7–23.
Sands P. (1995) Modelling canopy production. I. Optimal distribution of photosynthetic resources. *Australian Journal of Plant Physiology*, 22, 593–601.
Scartazza A., Di Baccio D., Bertolotto P., Gavrichkova O. & Matteucci G. (2016) Investigating the European beech (*Fagus sylvatica* L.) leaf characteristics along the vertical canopy profile: leaf structure, photosynthetic capacity, light energy dissipation and photoprotection mechanisms. *Tree Physiology*, 36, 1060–1076.
Schimel J.P., Bilbrough C. & Welker J.M. (2004) Increased snow depth affects microbial activity and nitrogen mineralization in two Arctic tundra communities. *Soil Biology and Biochemistry*, 36, 217–227.
Schimel J.P. & Stuart Chapin F. (1996) Tundra plant uptake of amino acid and NH_4^+ nitrogen in situ: plants compete well for amino acid N. *Ecology*, 77, 2142–2147.
Schnieder C.A., Rasband W.S. & Eliceiri K.W. (2012) NIH image to ImageJ: 25 years of image analysis. *Nature Methods*, 9, 671–675.
Schulze E.D., Kelliher F.M., Körner C., Lloyd J. & Leuning R. (1994) Relationships among maximal stomatal conductance, ecosystem surface conductance, carbon assimilation rate and plant nitrogen nutrition: a global ecology scaling exercise. *Annual Review of Ecology and Systematics*, 25, 629–662.
Schuster W.S.F., Griffin K.L., Roth H., Turnbull M.H., Whitehead D. & Tissue D.T. (2008) Changes in composition, structure and above-ground biomass over seventy-six years (1930–2006) in Black Rock Forest, Hudson Highlands, southeastern New York State. *Tree Physiology*, 28, 537–549.
Sellers P.J., Berry J.A., Collatz G.J., Field C.B. & Hall F.G. (1992) Canopy reflectance, photosynthesis, and transpiration. III. A reanalysis using improved leaf models and a new canopy integration scheme. *Remote Sensing of Environment*, 42, 187–216.
Sharp R.E., Matthews M.A. & Boyer J.S. (1984) Kok effect and the quantum yield of photosynthesis: light partially inhibits dark respiration. *Plant Physiology*, 75, 95–101.
Slaughter C.W. & Viereck L.A. (1986) Climatic characteristics of the Taiga in interior Alaska. In: Van Cleve K., Chapin F.S. III, Flanagan P.W., Viereck L.A. & Dyrness C.T. (Eds.) *Forest ecosystems in the Alaskan Taiga: a synthesis of structure and function*. Springer, pp. 9–21.
Smith W.K., Vogelmann T.C., DeLucia E.H., Bell D.T. & Shepherd K.A. (1997) Leaf form and photosynthesis: do leaf structure and orientation interact to regulate internal light and carbon dioxide? *BioScience*, 47, 785–793.
ter Steege H. (1993) *HEMIPHOT, a programme to analyze vegetation indices, light and light quality from hemispherical photographs*. Tropenbos Foundation.
ter Steege H. (1997) Winphot, version 5.0. A programme to analyse vegetation indices, light and light quality from hemispherical photographs. Utrecht University, Utrecht: Tropenbos-Guyana Programme.
ter Steege H. (2018) Hemiphot.R: free R scripts to analyse hemispherical photographs for canopy openness, leaf area index and photosynthetic active radiation under forest canopies. Leiden, The Netherlands: Naturalis Biodiversity Center.
Tcherkez G., Gauthier P., Buckley T.N., Busch F.A., Barbour M.M., Bruhn D. et al. (2017) Tracking the origins of the Kok effect, 70 years after its discovery. *New Phytologist*, 214, 506–510.
Thompson R.S., Anderson K.H., Pelltier R.T., Strickland L.E., Shafer S.L., Bartlein P.J. & McFadden A.K. (2015) Atlas of relations between climatic parameters and distributions of important trees and shrubs in North America: revisions for all taxa from the United States and Canada and new taxa from the western United States Professional Paper. https://doi.org/10.3133/pp1650g
Valladares F. & Niinemets U. (2008) Shade tolerance, a key plant feature of complex nature and consequences. *Annual Review of Ecology, Evolution, and Systematics*, 39, 237–257.
Viereck L.A., Van Cleve K. & Dyrness C.T. (1986) Forest ecosystem distribution in the taiga environment. In: Van Cleve K., Chapin F.S. III, Flanagan P.W., Viereck L.A. & Dyrness C.T. (Eds.) *Forest ecosystems in the Alaskan Taiga: a synthesis of structure and function*. Springer, pp. 22–43.
Whitehead D., Griffin K.L., Turnbull M.H., Tissue D.T., Engel V.C., Brown K.J. et al. (2004) Response of total night-time respiration to differences in total daily photosynthesis for leaves in a *Quercus rubra* L. canopy: implications for modelling canopy CO_2 exchange. *Global Change Biology*, 10, 925–938.

13653040, 2023, 1, Downloaded from https://onlinelibrary.wiley.com/doi/10.1111/pce.14448 by Columbia University Libraries, Wiley Online Library on [05/09/2024]. See the Terms and Conditions (https://onlinelibrary.wiley.com/terms-and-conditions) on Wiley Online Library for rules of use; OA articles are governed by the applicable Creative Commons License

Wong C.Y.S. & Gamon J.A. (2015a) Three causes of variation in the photochemical reflectance index (PRI) in evergreen conifers. *New Phytologist*, 206, 187–195.

Wong C.Y.S. & Gamon J.A. (2015b) The photochemical reflectance index provides an optical indicator of spring photosynthetic activation in evergreen conifers. *New Phytologist*, 206, 196–208.

Wong S.C., Cowan I.R. & Farquhar G.D. (1978) Leaf conductance in relation to assimilation in *Eucalyptus pauciflora* Sieb. ex Spreng: influence of irradiance and partial pressure of carbon dioxide. *Plant Physiology*, 62, 670–674.

Yamori W. & von Caemmerer S. (2009) Effect of rubisco activase deficiency on the temperature response of CO_2 assimilation rate and rubisco activation state: insights from transgenic tobacco with reduced amounts of rubisco activase. *Plant Physiology*, 151, 2073–2082.

Yin X. (1993) Variation in foliar nitrogen concentration by forest type and climatic gradients in North America. *Canadian Journal of Forest Research*, 23, 1587–1602.

Zweifel R., Böhm J.P. & Häsler R. (2002) Midday stomatal closure in Norway spruce—reactions in the upper and lower crown. *Tree Physiology*, 22, 1125–1136.

SUPPORTING INFORMATION

Additional supporting information can be found online in the Supporting Information section at the end of this article.

How to cite this article: Schmiege, S.C., Griffin, K.L., Boelman, N.T., Vierling, L.A., Bruner, S.G., Min, E. et al. (2023) Vertical gradients in photosynthetic physiology diverge at the latitudinal range extremes of white spruce. *Plant, Cell & Environment*, 46, 45–63. https://doi.org/10.1111/pce.14448

13653040, 2023, 1, Downloaded from https://onlinelibrary.wiley.com/doi/10.1111/pce.14448 by Columbia University Libraries, Wiley Online Library on [05/09/2024]. See the Terms and Conditions (https://onlinelibrary.wiley.com/terms-and-conditions) on Wiley Online Library for rules of use; OA articles are governed by the applicable Creative Commons License